

# Opto-Electronic Advances

CN 51-1781/TN ISSN 2096-4579 (Print) ISSN 2097-3993 (Online)

## Advances and new perspectives of optical systems and technologies for aerospace applications: a comprehensive review

Sandro Oliveira, Jan Nedoma, Radek Martinek and Carlos Marques

**Citation:** Oliveira S, Nedoma J, Martinek R, et al. Advances and new perspectives of optical systems and technologies for aerospace applications: a comprehensive review. *Opto-Electron Adv* 8, 250036(2025).

<https://doi.org/10.29026/oea.2025.250036>

Received: 3 March 2025; Accepted: 29 May 2025; Published online: 16 July 2025

## Related articles

### Specialty optical fibers for advanced sensing applications

Huanhuan Liu, Dora Juan Juan Hu, Qizhen Sun, Lei Wei, Kaiwei Li, Changrui Liao, Bozhe Li, Cong Zhao, Xinyong Dong, Yuhan Tang, Yihong Xiao, Gerd Keiser, Perry Ping Shum

*Opto-Electronic Science* 2023 2, 220025 doi: [10.29026/oes.2023.220025](https://doi.org/10.29026/oes.2023.220025)

### Wearable photonic smart wristband for cardiorespiratory function assessment and biometric identification

Wenbo Li, Yukun Long, Yingyin Yan, Kun Xiao, Zhuo Wang, Di Zheng, Arnaldo Leal-Junior, Santosh Kumar, Beatriz Ortega, Carlos Marques, Xiaoli Li, Rui Min

*Opto-Electronic Advances* 2025 8, 240254 doi: [10.29026/oea.2025.240254](https://doi.org/10.29026/oea.2025.240254)

More related article in Opto-Electronic Journals Group website 

 Opto-Electronic  
Advances

<http://www.oejournal.org/oea>



 OE\_Journal



 @OptoElectronAdv

DOI: [10.29026/oea.2025.250036](https://doi.org/10.29026/oea.2025.250036)CSTR: [32247.14.oea.2025.250036](https://cstr.net/urn:cstr:32247.14.oea.2025.250036)

# Advances and new perspectives of optical systems and technologies for aerospace applications: a comprehensive review

Sandro Oliveira<sup>1</sup>, Jan Nedoma<sup>2</sup>, Radek Martinek<sup>3</sup> and Carlos Marques<sup>1,4\*</sup>

The aerospace industry is a very unforgiving field, where even the smallest error could have catastrophic consequences. To reduce the risk of disaster, multiple systems are put into place to provide accurate information for informed decision making. The field of optics has played a pivotal role in advancing space exploration and technology. From enabling precise observations of distant celestial objects to facilitating communication across vast interstellar distances, optics has become an indispensable tool in space science and supported by significant advances in the last few years, new and improved applications continue to arise. This review aims to explore the diverse applications of optical systems and technologies in the aerospace industry, highlighting recent developments regarding navigation, communications, process and structural health monitoring, as well as the monitorization of astronauts' health.

**Keywords:** astronaut well-being; structural health monitoring; navigation and optical communication in space

Oliveira S, Nedoma J, Martinek R et al. Advances and new perspectives of optical systems and technologies for aerospace applications: a comprehensive review. *Opto-Electron Adv* 8, 250036 (2025).

## Introduction

The aerospace industry, which encompasses commercial and military aircraft, space launch and in-space systems, missiles, satellites and general aviation, aims to develop not only a cleaner means of transport, but also reduce its associated operating costs<sup>1</sup>. The economic pressure resulting from rising fuel prices in addition to government-mandated environmental rules have motivated researchers to focus on ways to create lighter and more efficient aircraft, as fuel consumption is significantly reduced by using lightweight alloys<sup>2</sup>.

Advances in aerospace systems are strongly dependent on advances in materials and processing technologies. Modern components are being projected to be more durable, efficient and have better performances. For example, gas turbine engines for aircraft are being designed to run at higher pressures and temperatures to generate more thrust. Similar considerations apply to spacecraft, where in-space propulsion and power systems are key components enabled through the innovation in material science<sup>3</sup>.

Although aluminum has been considered the primary

<sup>1</sup>CICECO-Aveiro Institute of Materials, Physics Department, University of Aveiro, 3810-193 Aveiro, Portugal; <sup>2</sup>Department of Telecommunications, VSB-Technical University of Ostrava, Ostrava 70800, Czech Republic; <sup>3</sup>Department of Cybernetics and Biomedical Engineering, VSB-Technical University of Ostrava, Ostrava 70800, Czech Republic; <sup>4</sup>Department of Physics, VSB-Technical University of Ostrava, Ostrava 70800, Czech Republic.

\*Correspondence: C Marques, E-mail: [carlos.marques@ua.pt](mailto:carlos.marques@ua.pt)

Received: 3 March 2025; Accepted: 29 May 2025; Published online: 16 July 2025



**Open Access** This article is licensed under a Creative Commons Attribution 4.0 International License.

To view a copy of this license, visit <http://creativecommons.org/licenses/by/4.0/>.

© The Author(s) 2025. Published by Institute of Optics and Electronics, Chinese Academy of Sciences.

material for aerospace applications, there has been a significant demand for new materials that are high-strength, lightweight, non-corrosive, recyclable, and ultra-violet and impact resistant<sup>4</sup>. In particular, the use of composite laminates has increased greatly in the last years. Natural composites (such as wood and fabrics) have found applications in aircraft from the first flight of the Wright Brothers' Flyer 1. With the years, more robust materials were being developed, and the discovery of carbon fiber at the royal aircraft establishment at Farnborough, UK, in 1964 marks the first step towards their major contribution to aircraft structures<sup>5</sup>. Carbon fiber reinforced polymers (CFRP), and also glass fiber reinforced polymers (GFRP), possess remarkable thermal-mechanical properties such as high specific strength and stiffness, as well as being lightweight, corrosion resistant and thermal insulators<sup>6</sup>. Given these remarkable properties, these materials have been applied to engine casings, wing sections, tail plane, fuselage and control surfaces, and it is estimated that composite materials represent around 50% of the weight of current aircraft, such as Boeing 787 and Airbus 350, whose main frames, fuselage/wing skins and associated stringers are manufactured by CFRP<sup>7,8</sup>.

This shift into composite materials has created a need for lightweight sensors and cabling that are immune to electromagnetic interference. Multiple sensing parameters are required in the aerospace industry and research, including strain, temperature, pressure, acceleration, and vibration, among others, which must be evaluated at multiple steps in the lifecycle of a component, from its fabrication to the testing and onboard missions<sup>9</sup>.

The type of sensor to be implemented heavily depends on the measurand as well as the intended application. Both aircraft and spacecraft need to be carefully tailored for their intended missions and required lifetime, spanning from material choice to design and the final manufacturing process. Closely monitoring these systems is critical to ensure a successful operation. The specifications for any sensor are derived from the type of mission, namely altitude, operational lifetime, location in the craft and intended measurement parameters<sup>10</sup>.

Space remains a great frontier of development, as it can be seen as the most unforgiving type of environment to explore. One significant challenge inherent to the space environment is the vacuum. Considering missions that occur on the so-called Low Earth Orbit (LEO) at around 200 and 1000 km in altitude, spacecraft need to be able to

withstand  $10^{-9}$ – $10^{-11}$  Torr (1 Torr  $\approx 1.333 \times 10^2$  Pa) on the outside<sup>11</sup>. At these altitudes, thermal cycling is also concerning, where temperatures can rapidly oscillate between 100 °C and –100 °C<sup>12</sup>. Adding to the harsh conditions of space, both UV and charged particle (ionizing) radiation effect the integrity of the materials. Considering missions at the altitude of the ISS, astronauts are exposed to an annual dose-equivalent of about 0.3 Sv<sup>13</sup>, and this value increases as destinations extend farther from Earth. It is estimated that astronauts embarking on future exploration missions to Mars will receive an estimated 1 Sv of radiation during a round trip<sup>26</sup>. These values greatly exceed the typical annual dose the general population on Earth is exposed to (1 mSv). Furthermore, the threat of impact also needs to be carefully considered. In LEO, the typical velocities of space debris range from about 7 to 10 km/s<sup>14</sup>, and even relatively small particles, with sizes spanning from approximately 10  $\mu\text{m}$  to a few millimeters, can generate sufficiently high impact energies to damage orbiting spacecraft. significant risk to both the structural integrity and operational performance of the systems<sup>15</sup>. From a logistic standpoint, one of the greatest challenges in space system design is managing size and weight constraints. Every gram saved translates to reduced fuel consumption and lower launch costs, making miniaturization a priority. The goal is to shrink components without compromising performance, allowing for more efficient payload allocation and the integration of additional systems that would otherwise be unfeasible<sup>16</sup>.

Given these harsh conditions, the design and planning of aerospace optical systems needs to address some inherent critical factors to ensure optimal performance and reliability in extreme environments. Optical aberrations, such as spherical aberration, can degrade image quality and must be accounted for through precise optical design, advanced mathematical modeling, and high-precision manufacturing techniques<sup>16</sup>. Thermal effects pose another major consideration, as temperature fluctuations can cause material expansion, optical misalignment, and birefringence, requiring careful material selection, thermal compensation strategies, and structural design adjustments to maintain system stability<sup>17</sup>. Mechanical integration also demands attention at the planning stage, as maintaining optical alignment in aerospace platforms necessitates robust mounting structures, vibration isolation mechanisms, and stringent tolerance management. Additionally, contamination control must be integrated into the design process, as outgassing of materials

and residual particulates can degrade optical surfaces and impair system performance, necessitating strict cleanliness protocols from fabrication through operational deployment<sup>18</sup>. Addressing these challenges proactively in the early stages of system development is crucial to ensuring longevity, accuracy, and efficiency of aerospace optical technologies.

Despite these challenges, it is expected that the next decades will bring great developments, namely revolving around the implementation of automated, smart and reusable spacecraft, while guaranteeing proper health and safety conditions for the astronauts<sup>19,20</sup>. This can only be achieved through a network of robust sensing approaches that can withstand space's inherent harsh conditions, and the sizing constraints that space travel entails. The harsh conditions that air and spacecraft are subject to heavily condition the types of materials that may be used for aerospace applications. Although the effects these threats have on the materials vary greatly according to the materials themselves, their thickness, and stress levels, resistant materials need to be chosen to survive them. Also to be considered is the specific mission environment, including the altitude at which the materials are used and for how long they remain there<sup>21</sup>.

Given the challenging nature of space, the use of optics has some advantages over the use of other types of components. Optical signals are immune to electromagnetic interference (EMI), which can disrupt or degrade electrical signals in electronic circuits<sup>22</sup>.

Optical fibers, in particular, are especially attractive for these applications, as the need for lightweight and miniaturized systems is paramount. Optical fibers are intrinsically immune to electromagnetic interference, and are thus often deployed in harsh environments. They are also lighter than copper cables and allow the measurement of multiple parameters at once<sup>23</sup>.

The evolution of optical systems in aerospace has been marked by continuous advancements, driven by technological innovation and expanding mission requirements. In the 1940s and 1950s, early aerial reconnaissance cameras played a pivotal role in military surveillance, laying the foundation for airborne imaging. By the 1960s and 1970s, the advent of satellite imaging and infrared sensing revolutionized remote sensing, enabling more precise Earth observation and defense applications. The 1980s and 1990s introduced adaptive optics, significantly improving image resolution and leading to the launch of space telescopes such as Hubble, which transformed

our understanding of the universe. In the 2000s and 2010s, high-resolution satellite imaging and LIDAR technology enabled detailed terrain mapping and environmental monitoring<sup>10,24</sup>. Today, advancements in AI-driven image processing, miniaturization, and novel manufacturing techniques are pushing the boundaries of aerospace optics, enabling the development of more compact, efficient, and intelligent optical systems. This review highlights recent breakthroughs, emphasizing the interdisciplinary nature of optical technologies in aerospace applications.

## Applications of optical systems in aerospace engineering

Optical systems have the potential to continue to revolutionize the aerospace industry, offering significant advantages in areas such as communication, navigation, environmental sensing, and structural and human health. Multiple different technologies can be employed for this purpose, such as optical fiber-based sensing, laser technology or imaging systems, to name a few. This chapter explores recent advances on the application of optical systems across the aerospace sector, highlighting innovative technologies. At the end of this chapter, a comprehensive table (Table 1) summarizes the key research articles discussed, categorizing them by application to provide a clear reference for further study.

### Navigation

A robust identification of a vehicle's position is crucial for its navigation. Optical remote sensing cameras play an irreplaceable role in providing data for space altitude measurements and provide a visual perception for scientific research. With the recent advances in technology, the performance of optical remote sensing cameras has also increased greatly, with significant achievements being accomplished in temporal, spatial and spectral resolution. To reduce mass and thus reduce costs associated with fuel consumption, multispectral integrated optical systems have become a trend in deep space exploration, which refers to space activities that explore celestial bodies both in and beyond the solar system. This paper reports on designing and constructing a common-aperture multispectral imaging system that can simultaneously obtain ultraviolet, visible, mid-wave, and long-wave infrared wavebands<sup>25</sup>. This system had a full field-of-view of 6°, and a common entrance pupil with a diameter of 60 mm.

**Table 1** | Overview of optical systems recently reported in the literature for aerospace applications.

Ref	Year	Application	Results/Highlights	Testing conditions	Type
ref. <sup>25</sup>	2023	Navigation	Simultaneously obtain ultraviolet, visible, mid-wave, and long-wave infrared waveband information	Laboratory experiments (prototype)	Multispectral imaging system
ref. <sup>26</sup>	2022		Real-time display of different terrains' coordinate system	Laboratory experiments (prototype)	Vision-based electro-optical
ref. <sup>27</sup>	2022		Excellent crater detection on the moon (~3px)	Algorithm testing	Vision-based with convolutional neural network
ref. <sup>28</sup>	2018		Guidance and control of an unmanned helicopter	Laboratory experiments and real flight test	Optical and inertial sensors
ref. <sup>29</sup>	2017		Used in the controller to smoothly land a micro air vehicle	Laboratory experiments and real flight test	Optical flow monocular camera-based
ref. <sup>30</sup>	2022		Least-squares solution and analytical covariance to solve observer position	Analytical/ Numerical	Multiple beacons (line-of-sight)
ref. <sup>31,32</sup>	2021		Estimated position and velocity applied to the M-ARGO mission	Laboratory experiments and space deployment	Multiple beacons (line-of-sight)
ref. <sup>33</sup>	2023		"Absolute" pointing and accurate inertial angular rate Stabilized inertial reference unit	Laboratory experiments	Imaging system
ref. <sup>42</sup>	2024		Three orthogonal accelerometers and gyroscopes	Laboratory experiments (Scheduled space deployment)	Interferometric FBG
ref. <sup>46</sup>	2017	Temperature	Sensitivity of 25.8 pm/°C up to 1400 °C	Laboratory experiments	FBG
ref. <sup>47</sup>	2022		Maximum sensitivity of -850 pm/K between 100–200 K -170 pm/K at 20 K	Laboratory experiments	Long-period fiber gratings
ref. <sup>48</sup>	2022		Pre-tensioned fibers more accurate than free fibers	Laboratory experiments	FBG
ref. <sup>49</sup>	2022		Sensitivity 15.7 pm/°C between 100–1000 °C	Laboratory experiments	RFBG
ref. <sup>50</sup>	2018		Sensitivity of 10.54 pm/°C between -40 °C and 80 °C	Laboratory experiments	FBG
ref. <sup>51</sup>	2017		Tested on a rexus 22 sounding rocket	Laboratory experiments and rocket testing	FBG
ref. <sup>10</sup>	2021		Tested on satellite FP7 PEASSS Resistant up to 4 MGy	Laboratory experiments and satellite testing	FBG
ref. <sup>53</sup>	2023		Radiation	A linear response between 10 <sup>-3</sup> and 10 <sup>2</sup> Gy (SiO <sub>2</sub> )	Laboratory experiments
ref. <sup>54</sup>	2023	Lowest dose rate of 21 μGy (SiO <sub>2</sub> )/h		Laboratory experiments and CERN tests	RIA
ref. <sup>56</sup>	2018	Gas	Proof-of-concept to measure CO <sub>2</sub> during flight	Laboratory experiments	Absorption spectroscopy
ref. <sup>57</sup>	2018		CO, HCl, HCN, HF, CO <sub>2</sub> , and O <sub>2</sub> within critical levels, at pressures from 0.5 atm to 1 atm	Laboratory experiments	Absorption spectroscopy
ref. <sup>58</sup>	2020	Gas/PM	CO and CO <sub>2</sub> PM <sub>1</sub> , PM <sub>2.5</sub> , PM <sub>4</sub> , PM <sub>10</sub> and PM <sub>15</sub>	Laboratory experiments	Electrochemical and optical (spectroscopy-based)
ref. <sup>64</sup>	2018	Location	Extremely low resource optical identifier for low earth orbit objects	Laboratory experiments and flight test	Laser
ref. <sup>65</sup>	2022		Simultaneously determining precise orbits and identifying space objects	Laboratory experiments	Laser
ref. <sup>69</sup>	2024	Communication	Maximum downlink data-rate of 267 Mb/s	Aboard the Psyche spacecraft (NASA)	Laser
ref. <sup>74</sup>	2020		Qualification of waveguides fabricated in glass by femtosecond laser micromachining	Laboratory experiments	Integrated optics

**Table 1 (Continued)**

Ref	Year	Application	Results/Highlights	Testing conditions	Type
ref. <sup>85,86</sup>	2020 2018	Structural health monitoring	Determine cross-sectional forces and moments on wing	Laboratory experiments	FBG
ref. <sup>88</sup>	2024		Cantilever beam-based sensor for frequencies between 0 and 350 Hz	Laboratory experiments	FBG
ref. <sup>89</sup>	2020		Supports can be designed to resonate at a given frequency to increase sensitivity to small amplitude vibrations	Laboratory experiments Numerical simulation	FBG
ref. <sup>90</sup>	2024		Operating frequency range is 0–60 Hz, and sensitivity of 24.24 $\mu\text{m/g}$	Laboratory experiments Numerical simulation	FBG
ref. <sup>91</sup>	2021		Detection of BVID on CFRP laminates (wing structure) 34–46 thermoset and 70 mm thermoplastic	Laboratory experiments	FBG
ref. <sup>92</sup>	2019		Mean error for X coordinate is 18.36 mm and for Y coordinate is 21.88 mm, for location prediction	Laboratory experiments	FBG
ref. <sup>93</sup>	2020		Average localization error of 14.2 mm, with a training time of 0.7 s	Laboratory experiments	FBG
ref. <sup>94</sup>	2018		3-order sum of squares of deviations can predict the impact point better	Laboratory experiments	FBG
ref. <sup>95</sup>	2017		Resolution of the disbond detection was approximately 2 mm	Laboratory experiments	FBG
ref. <sup>96</sup>	2019		The sensors, packaging and installation were negligibly affected (temperature, pressure, humidity, etc)	Laboratory experiments (flight simulation)	FBG
ref. <sup>106</sup>	2016		Able to monitor crack growth and reconstruct the crack surfaces in GFRP and profilometry in CFRP	Laboratory experiments	OCT
ref. <sup>110,111</sup>	2014		Measuring 3D crack growth during delamination in GFRP	Laboratory experiments (Wind turbine)	OCT
ref. <sup>113</sup>	2023		Detect the most common defects in glass fiber reinforced tapes	Laboratory experiments	OCT
ref. <sup>119</sup>	2024		Measure defects in thermal barrier coatings (519 $\mu\text{m}$ depth and 100 $\mu\text{m}$ width)	Laboratory experiments	OCT/Terahertz pulsed imaging
ref. <sup>120</sup>	2020		Track the compression displacements in composite specimens	Laboratory experiments	OCT/Digital holographic interferometry
ref. <sup>123</sup>	2018	Astronaut's health	Portable system capable of measuring air temperature and pressure, flow rates, O <sub>2</sub> and CO <sub>2</sub>	Patented (NASA)	NDIR spectroscopy (CO <sub>2</sub> )
ref. <sup>127</sup>	2024		Miniature cytometry-based analyzer, modified to fit space travel	Onboard ISS	Flow cytometry (dual laser)
ref. <sup>129</sup>	2018		Analysis of morphological changes in the optic nerve head of 15 astronauts (pre and postflight)	Retrospective data (NASA)	OCT

The issue of navigation control is even more critical when it comes to autonomous vehicles. Vision sensors employ specific features within the camera's field-of-view to formulate object locations in the world and map them to the corresponding pixels in a 2-D image. A vision-based relative motion sensor called OptoNav (Optical Landing Navigation), was developed using low-cost optical components<sup>26</sup>. This system, which employed three laser altimeters and a camera, was shown to be able to aid the vehicle operator to land in a controlled manner.

Another paper presented a vision-based navigation system using a convolutional neural network and its application in a moon landing scenario<sup>27</sup>, whose crater detection delivered outstanding center localization results (below  $\sim 3$  px, on average) with respect to database ones.

The Autonomous Terrain-based Optical Navigation (ATON) project is a remarkable example of the applications of optical components for autonomous navigation, including an inertial measurement unit, a laser altimeter, a star tracker and navigation cameras. Within the scope

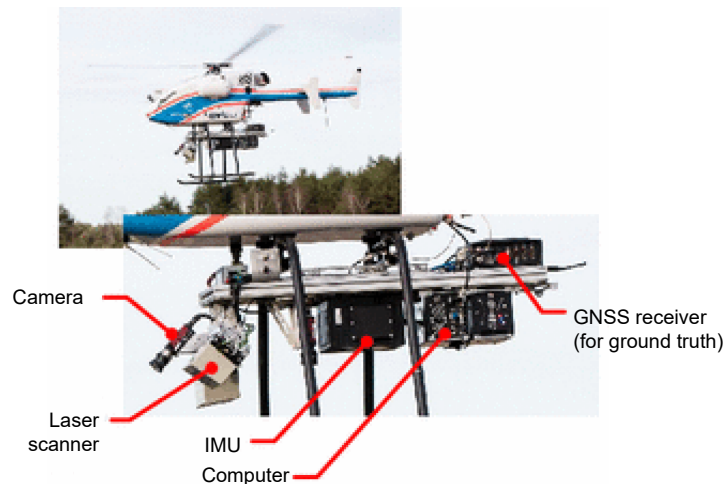


**Fig. 1 |** Setup used for the control of an unmanned helicopter under the ATON project, highlighting its most relevant components. Figure reproduced with permission from ref.<sup>28</sup>, Springer Nature.

of this project, different image processing techniques and optical navigation methods as well as sensor data fusion were developed. The developed system was tested on an unmanned helicopter, in place of the GPS-based standard navigation system (Fig. 1)<sup>28</sup>.

In recent years, micro air vehicles have become popular. However, due to their size and weight constraints, there needs to be a careful planning process for a limited amount of payload and sensors to be implemented, and the development of more robust algorithms. To address these concerns, and by taking inspiration from flying insects, an optical flow-based approach was developed<sup>29</sup>. Optical flow can be understood as the apparent visual motion of an object in reference to the observer, and this can be obtained using a monocular camera. Thus, one can obtain information regarding both velocity and distance to the object the camera captures. This team developed an algorithm that allowed them to accurately estimate the velocity of a test drone, and also land it smoothly, even in windy conditions.

This interest in miniaturization also extends to interplanetary spacecraft, which, coupled with constant technological advances, has resulted in an increase in the number of satellites being launched into space. This has caused a problem for ground facilities that relied on traditional radiometric tracking. Autonomous navigation has been proposed as a solid alternative to enable a sustainable deep-space exploration. This paper tackled the deep-space optical navigation problem, which consists of the estimation of an observer position exploiting the line-of-sight (LOS) directions to a number of objects, or beacons, acquired by on-board optical sensors such as

navigation camera and star trackers. This team focused on the use of multiple beacons to derive the least-squares solution and analytical covariance<sup>30</sup>.

CubeSats is an example of a class of nanosatellites with standardized measurements, where 1U equals a cube with a 10 cm edge. M-ARGO, the 'Miniaturized-Asteroid Remote Geophysical Observer', is European Space Agency's first stand-alone CubeSat mission for deep space, and consists of determining the spacecraft state in deep space by tracking the LOS directions to a number of known navigation beacons. The LOS directions are acquired for one beacon at a time using available miniaturized optical sensors and are given as input to a Kalman filter<sup>31</sup>. It is important to note that the accuracy (under good observation conditions) in terms of position and velocity reaches values of 1000 km and 0.1 m/s. Different strategies have been adopted to enhance the solution accuracy of the autonomous navigation problem for deep-space CubeSats, either through the optimal beacons selection method or by introducing light effects corrections inside the model equations. A detailed overview of this problem can be found in ref.<sup>32</sup>.

Precision line-of-sight control is also essential for defense applications, namely where sub-microradian to microradian pointing accuracies are required against dynamic targets. This paper<sup>33</sup> addressed these particular challenges, comparing the tradeoffs between stable platform and strapdown stabilization mechanizations. Even though both are made up of gyro sensors and accelerometers and include an optical reference for alignment, only in the stable platform is the optical reference stabilized. This system can become a stabilized inertial

reference unit, providing a stabilized optical reference for the pointing and control systems. The authors reported a gyroscope angle error as small as  $(0.05\text{--}1.0) \times 10^{-6}$  rad.

Gyroscopes are a requirement for many missions and are used for maintaining the attitude and orbital control of spacecraft. Optical fiber gyroscopes (FOGs), in particular, have become essential for spacecraft navigation and attitude control, offering high precision, reliability, and resistance to environmental disturbances. Their development stems from the Sagnac effect, first demonstrated in 1913, which describes how rotational motion induces a phase shift in counter-propagating light beams within a closed-loop optical system. In the absence of rotation, the resulting interference fringes are stationary, however, their position shift according to the angular velocity of the system<sup>34</sup>. While early spacecraft relied on mechanical gyroscopes, the emergence of FOG technology in the 1970s and 1980s provided a superior alternative, eliminating moving parts and reducing power consumption, while having shorter reaction times and a higher accuracy<sup>35–37</sup>. The first in-space demonstration of an optical gyroscope occurred aboard NASA's X-ray Timing Explorer (1995–2012), validating its feasibility for space applications. Since then, advancements in radiation-hardened fiber optics and miniaturized designs have led to the development of space-qualified FOGs, such as VOBIS, which is optimized for long-duration missions in deep space and geostationary orbits<sup>38</sup>. The system demonstrated an in run bias stability better than 0.03 deg/hr, and the tests showed no degradation of VOBIS accuracy parameters after a 21 month flight. Today, FOGs are integral to spacecraft like the International Space Station (ISS), satellites, and planetary exploration probes, ensuring precise orientation and stability in the harsh conditions of space.

FOGs use special fibers, such as rare-Earth doped optical fibers (REDFs), which, coupled with an accelerometer, can provide rotational speed measurements and inertial positioning. While commonly used for navigation on earth, their advantages have been leveraged for many state-of-the-art satellites, such as Attitude and Orbit Control System (AOCS) for planetary landing or for electric propulsion and deep space exploration. Another example is a microsatellite, the SLOSHSAT-FLEVO (Sloshsat Facility for Liquid Experimentation and Verification in Orbit), launched to investigate the dynamics of fluids in microgravity, which integrates a 3-axis FOG<sup>39</sup>.

Efforts have been made to improve the effectiveness of

FOG. To amplify the Sagnac effect, FOGs use several kilometers of fiber per coil, which increases the vulnerability to radiation, as the radiation-induced attenuation effects quickly escalate at these lengths. Additionally, due to the rare-earth doping, the fibers (typically erbium-doped), are more sensitive to radiation. To mitigate this, radiation hardening strategies are crucial, and their effectiveness has already been demonstrated in satellites such as the Planck or Galileo<sup>40</sup>. Other efforts have been made to decrease associated costs. For example, Nunes and Sakamoto developed a passive FOG configuration that does not require modulation<sup>41</sup>.

Coupled with gyroscopes, accelerometers are also particularly useful in aerospace applications. Sakamoto et al. reported an optic inertial measurement unit, comprising three orthogonal closed-loop interferometric FOGs and a triaxial fiber optic accelerometer for determination of attitude and heading in 3D-space<sup>42</sup>. The developed system was reported by the group to be in-line with the currently available FOGs and to be the first triaxial accelerometer version able to accurately measure acceleration in the three axes. Additionally, the developed system is set to be deployed in space in July 2025, on board of a satellite launch rocket, which will allow the evaluation of performance in real space conditions.

## Environmental monitoring

### Temperature

Aerospace vehicles, especially aircraft, are subjected to both extremely high and low temperatures, ranging between  $-150$  °C to  $2000$  °C. However, the available un-packaged commercial fibers used for temperature sensing cannot typically withstand such high temperatures. However, they have been demonstrated to work on extreme conditions, such as monitoring heat pipes<sup>43</sup>. Thus, new approaches need to be implemented to use optical fibers as sensors for these applications.

New packaging designs have been developed in the last years to increase the maximum operating temperature of these sensors, such as employing sapphire-based fibers with femtosecond written gratings<sup>44</sup>. Sapphire fibers are remarkable for this kind of application due to this material's high melting point of  $2045$  °C<sup>45</sup>, which has resulted in the development of temperature sensors able to withstand temperatures higher than  $1400$  °C<sup>46</sup>. On the opposite side of the spectrum, this type of sensor has shown stability at low temperatures, having already been

proposed for cryogenic applications<sup>47</sup>.

Fiber Bragg gratings are especially useful for temperature sensing, and a lot of work has been done to verify their stability, accuracy, and sensitivity to operating conditions. The authors of ref.<sup>48</sup> evaluated the influence of two different methods of FBGs surface application have been considered (gluing with pre-tensioning vs. non-tensioned bonding).

On top of being lightweight, another great advantage of optical fiber systems is the possibility of simultaneously measuring more than one parameter at the same time. Tian et al. reported a system made up of two RFBGs for precise temperature and strain measurements under high temperature environments. While one RFBG was sensitive to both strain and temperature, the other was made insensitive to the applied strain. Results indicated a linear response between 100 °C and 1000 °C with the same sensitivity of ~ 15.7 pm/°C for both RFBGs<sup>49</sup>.

To fully adopt this type of sensing in space applications, it is also crucial to ensure that the sensors are able to not only withstand the extreme temperatures, but also work properly in a vacuum. To overcome the lack of convection in these conditions, in an effort to enhance the heat conduction speed of the sensor, a team developed a new type of package for an FBG temperature sensor, which included quartz powder and modified resin as fillers and adhesive to ensure stability<sup>50</sup>. Experiments show that the sensor developed has faster response speed (<3.3 s) and could reach temperature resolution of 0.095 °C.

Regarding the specific application of optical sensors for monitoring temperature in aerospace systems, there have been reports on certain elements of antennas, where temperature monitoring is important for early detection

of design problems. However, this is a challenging environment because of the radio frequency, which inhibits the use of conventional sensors such as thermocouples or thermistors. Thanks to their inherent immunity to electromagnetic interference, FBG sensors are an ideal option. This type of approach was demonstrated in two antenna samples (Fig. 2): a stripline Wilkinson divider breadboard used for the center divider of the NAVANT (transmit antenna for GALILEO system) and a 1:3 Divider used in a NASA's Mars ROVER antenna<sup>51</sup>.

Other report delves into the advantages of multiplexing provided by FBG sensors, when compared with thermistors, for the temperature measurement in a satellite's communication and service modules<sup>52</sup>. For example, the Geosynchronous Telecommunication Satellite EUROSTAR3000 (EADS ASTRIUM's satellite) requires temperature reading on more than 180 locations, so the use of FBG sensors results in a 74% decrease in mass, and cable length needed, from over 350 m to less than 100 m, while also improving time for installation. Another successful example is the European FP7 PEASSS (Piezoelectric Assisted Smart Satellite Structure) project that created a 3U CubeSat with an FBG interrogator and 6 FBG sensors for strain and temperature sensing. It was demonstrated to work and resist without problems up to 4 MGy<sup>10</sup>.

## Radiation

Dosimetry, the measurement of ionizing radiation dose absorbed by matter or tissue, is of special interest for space applications, where different types of particles, broad energy spectra and solar activity need to be accounted for. Optical fibers have been used for these

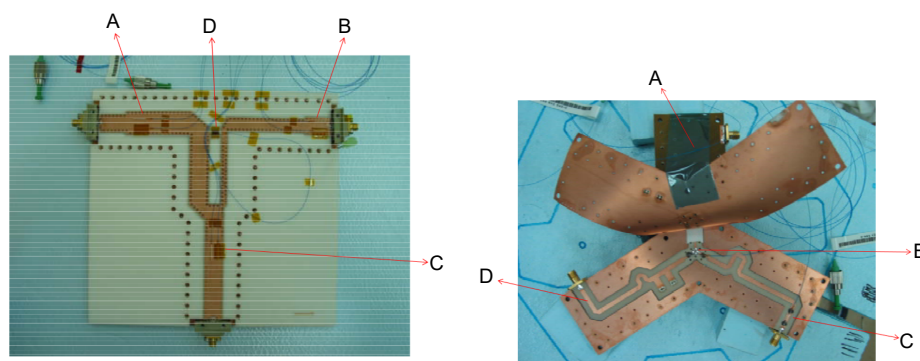


**Fig. 2 |** Left-FBG sensors on a Wilkinson divider from GALILEO's NAVANT antenna: (a) Input port of the Wilkinson divider. (b) Output ports of the divider. (c) Region with embedded FBG sensors. (d) Surface-mounted FBG sensors. Right-FBG sensors on a Mars ROVER divider sample: (A) Central connector or mechanical mount point; (B) Output lines or transmission lines. (C) Surface area with FBG sensors. (D) Embedded or internal sensing path. Figure reproduced with permission from ref.<sup>51</sup>, under a Creative Commons Attribution License.

applications. Meyer et al. proposed a phosphorus-doped, single-mode optical fiber dosimeter, with an embedded interrogator operating at 1610 nm<sup>53</sup>. While under  $\gamma$ - and X-rays, the proposed system evidenced a linear response between  $10^{-3}$  and  $10^2$  Gy(SiO<sub>2</sub>), with a performance comparable to other standard-sized systems.

Optical fiber-based dosimeters have already been deployed on the International Space Station, under the scope of the LUMINA project (Fig. 3). P-doped fibers were used for this purpose, and before deployment, a theoretical model was developed and experimental tests were carried out at CERN, which allowed for the calibration curve of the flight model to be obtained<sup>54</sup>.

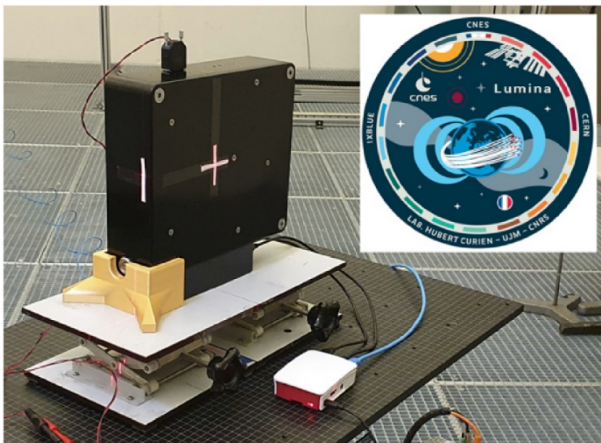


**Fig. 3** | LUMINA dosimeter during the experimental tests at CERN. Figure reproduced with permission from ref.<sup>54</sup>, under the terms of the Optica Open Access Publishing Agreement.

### Gas and particulate matter (PM)

Even though most materials used in the interior of manned spacecraft are non-flammable, they still produce smoke when overheated. Fires can reveal catastrophic to spacecraft due to the very limited options to extinguish them, so detectors should be able to detect smoke generated by oxidative pyrolysis (such as smoldering). As spacecraft fires differ greatly from those on the ground, as evidenced by a study performed on the International Space Station<sup>55</sup>, smoke detectors need to be optimized for this particular environment. A robust system of small and low-power sensors capable of measuring different key compounds could allow early detection and location of fires which in turn would allow early deployment of fire suppressants.

Absorption spectroscopy can be used to detect and quantify the concentration of various gases relevant to

combustion and pyrolysis, as they have absorption features in the mid-infrared range. Terracciano et al. designed and tested a CO<sub>2</sub> sensor, based on a 4.2  $\mu$ m light-emitting diode<sup>56</sup>. Through amplitude modulation it was possible to obtain species concentration, and frequency modulation revealed the ambient temperature. The system was tested with total pressures between 10.1 kPa and 101 kPa. The authors also suggest that the same principle could be applied to other hazardous gases.

The combustion Product Monitor is another example of absorption spectroscopy, this time using a tunable laser. This six-channel system was developed as part of the Spacecraft Fire Safety Demonstration (Saffire) Project, intended to measure concentrations of the target gases during low-gravity, reduced pressure oxidative pyrolysis of relevant test materials aboard a transfer vehicle returning from low Earth orbit. Available results showed the system was capable of measuring gas-phase concentrations of CO, HCl, HCN, HF, CO<sub>2</sub>, and O<sub>2</sub> within the critical levels, at pressures from 0.5 atm to 1 atm<sup>57</sup>.

This paper<sup>58</sup> delved into the performance evaluation of gas and particle sensors when applied to the detection of combustions of three commonly used spacecraft materials: cotton lamp wick, Nomex fabric, and Poly(methyl methacrylate) (PMMA). The system used included a variety of sensors, including a CO<sub>2</sub> analyzer by non-dispersive infrared, and four light scattering-based equipment's for the quantification of particulate matter of different sizes (PM<sub>1</sub>, PM<sub>2.5</sub>, PM<sub>4</sub>, PM<sub>10</sub> and PM<sub>15</sub>) (Fig. 4). CO<sub>2</sub> alone is not a good fire indicator, as human breath can cause some false positives, and some burning scenarios cause CO<sub>2</sub> levels only slightly above normal. However, results showed that PM sensors were responsive to both smoldering and flaming smoke, and that the low-cost options were sensitive enough to detect smoke.

### Location and imaging

Optical imaging systems have been instrumental in space exploration, with telescopes playing a crucial role in observing celestial phenomena and advancing our understanding of the universe<sup>59,60</sup>. Since the launch of the Hubble Space Telescope (HST) in 1990, space telescopes have provided high-resolution images of distant galaxies, refined estimates of the universe's age, and confirmed the presence of dark energy. The James Webb Space Telescope (JWST), launched in 2021, represents the next leap in space-based observatories, utilizing a 6.5 m primary mirror and infrared imaging capabilities to study the

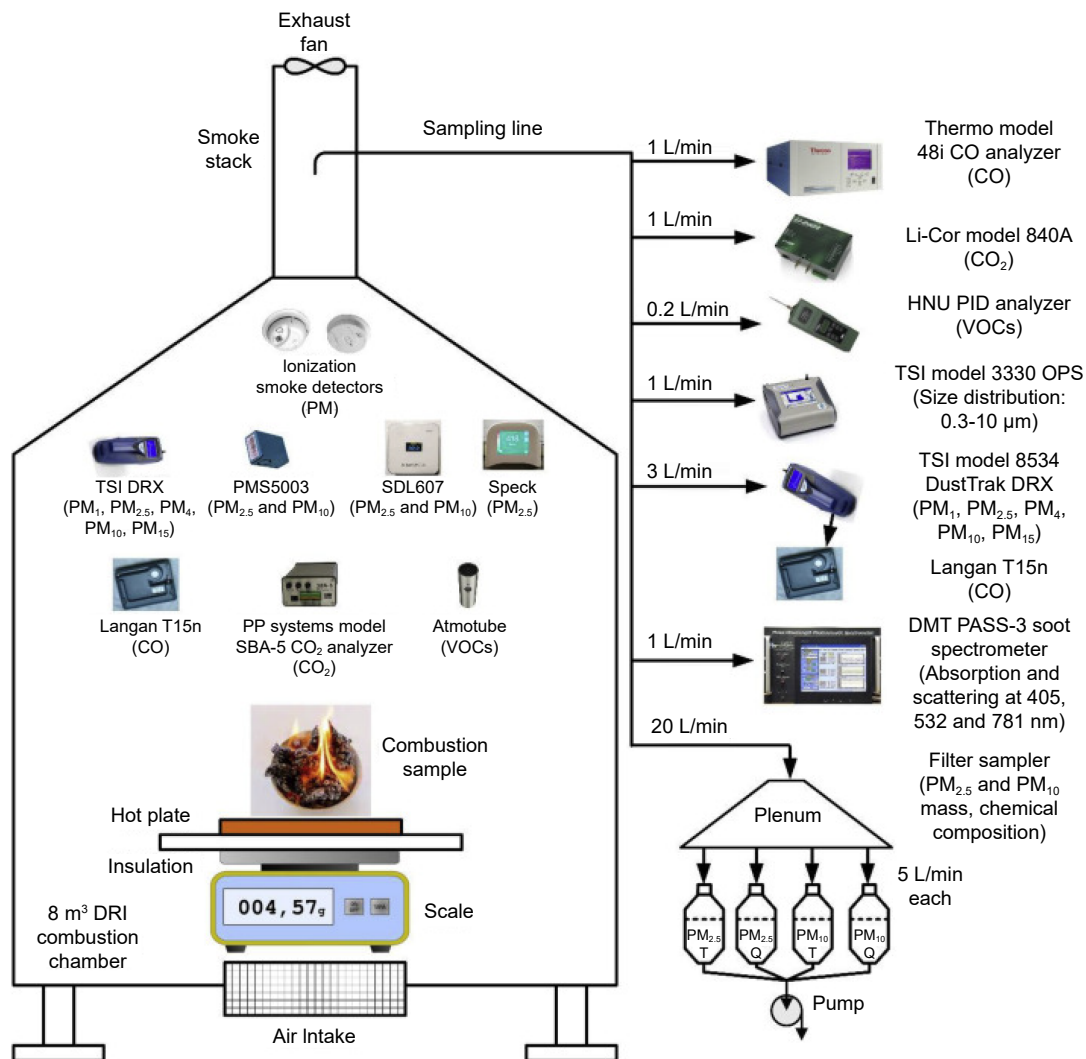


**Fig. 4 |** Experimental setup of the combustion experiment used to test the particulate matter evaluation system. Figure reproduced with permission from ref.<sup>58</sup>, Elsevier.

formation of the earliest galaxies and analyzing exoplanet atmospheres beyond the capabilities of visible-light telescopes<sup>61</sup>.

Building upon these advancements, a revolutionary electro-optical (EO) imaging sensor has been proposed, replacing conventional telescopes with photonic integrated circuits (PICs). This approach integrates millions of direct-detection white-light interferometers onto a single chip, eliminating the need for large optical elements while maintaining high-resolution imaging. Fabricated using CMOS-compatible photonic technologies, this system offers a scalable and cost-effective solution for future NASA missions, enabling a large-aperture, wide-field EO imager with significantly reduced mass and volume. Innovations in photonic interferometry hold the potential to transform space-based imaging,

making deep-space observations more accessible and efficient.

In addition to astronomical imaging, optical sensors are playing an increasingly important role in on-orbit servicing (OOS) and space traffic management<sup>62</sup>. Active sensors such as LiDAR, laser rangefinders, and microwave radars provide range and angle measurements, while visible-light and infrared cameras enhance high-resolution imaging for autonomous docking and inspection<sup>61</sup>. However, challenges such as target motion, limited observation windows, and resource constraints necessitate the continued refinement of these technologies. The integration of machine learning algorithms and multimodal sensor fusion is expected to further enhance autonomous spacecraft operations in future missions. The rapid rise in satellite launches, from approximately 100

in 2010 to over 1,000 annually by 2020, has resulted in growing congestion in low Earth orbit (LEO). This increase is driven by advances in miniaturization and cost-effective satellite manufacturing, leading to both higher space traffic and a rising density of space debris<sup>63</sup>. Efficient space traffic management is now critical, and the identification of satellites and debris is the first fundamental step.

Current identification methods rely primarily on RADAR and optical observations, but many objects in LEO remain unidentifiable. Alternative approaches include equipping satellites with identification hardware, such as the extremely low-resource optical identifier a "license plate" consisting of an array of laser diodes, which emits an optical signal that can be received and decoded on Earth<sup>64</sup>. However, this active technique requires additional power, making it impractical for non-operational satellites. Passive techniques, which do not require an external power source, are increasingly attractive. These methods often involve retroreflecting tags that remain functional even after a satellite's operational lifespan. A promising approach is satellite laser ranging

(SLR), where satellites are equipped with retroreflectors that reflect ground-based laser pulses for precise tracking. Bartels et al. proposed an advanced polarization-modulated SLR system, where specially designed retroreflectors alter the polarization state of received photons before reflecting them back to Earth, enhancing identification accuracy (Fig. 5)<sup>65</sup>.

Additionally, advancements in stray light (SL) management are improving optical system performance in space. Traditional SL characterization methods struggle to isolate individual contributors, limiting optical refinements. Recent research has introduced ultrafast time-of-flight (ToF) imaging, utilizing a pulsed laser and a streak camera to map and differentiate SL components based on their optical path lengths (OPL). This technique enables reverse engineering of SL origins, leading to more effective mitigation strategies and enhanced optical precision in space telescopes and EO sensors<sup>66</sup>.

Finally, progress in synthetic aperture radar (SAR) processing is further refining spaceborne imaging. A novel floating-point imaging chip based on system-on-chip (SoC) architecture has been developed for

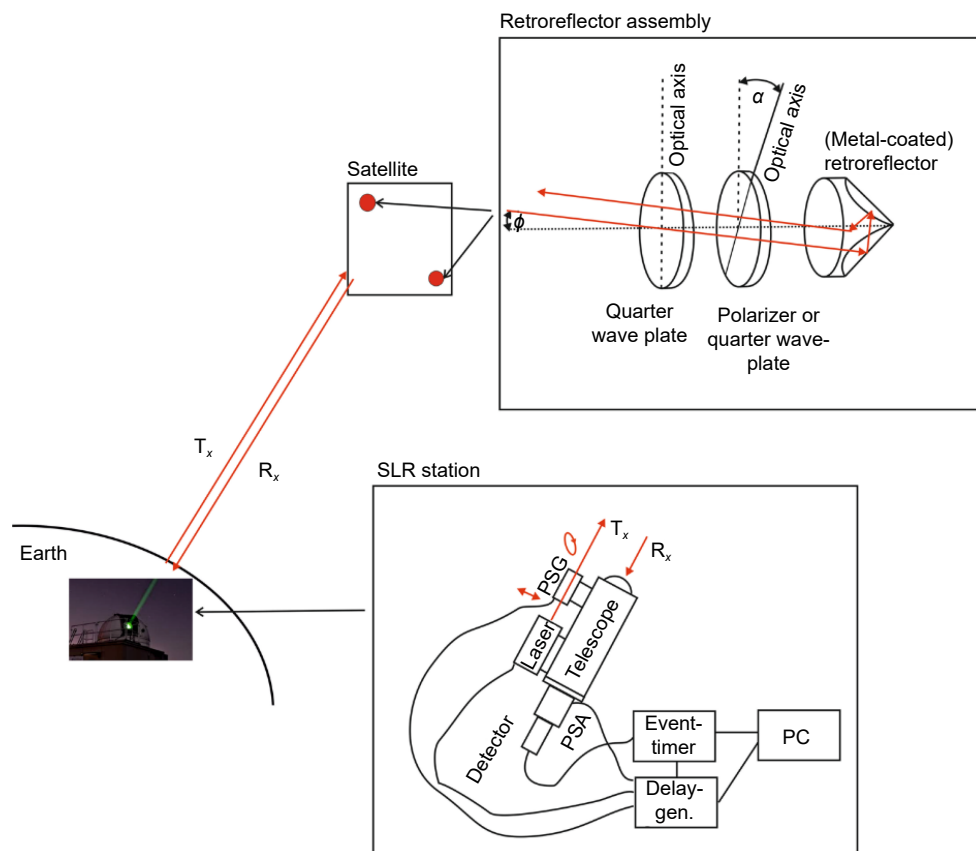


**Fig. 5 |** Schematic setup for polarization-modulated SLR. Figure reproduced with permission from ref.<sup>65</sup>, under a Creative Commons Attribution License.

multi-mode SAR imaging tasks. This system incorporates fault-tolerant techniques, such as fixed-point pipelined FFT processors, error correction codes (ECCs), and partial triple modular redundancy (PTMR), achieving real-time performance with low power consumption and high reliability. The system processes SAR raw data at 6.9 W, demonstrating significant improvements in computational efficiency and resilience to radiation effects, making it a viable candidate for long-term space missions<sup>65</sup>.

### Communications

In the past few years, tremendous growth has been experienced in the information and communication field, which has been accompanied by an intense growth in data, leading to congestion in the tried-and-tested radio frequency communications. Optical communication has arisen as a fitting alternative, offering much higher bandwidth, ease of deployment, unlicensed spectrum allocation, reduced power consumption and size, and improved security<sup>67</sup>.

This same problem also translates into deep space communications. At the same time as radio frequency communication is reaching its bandwidth limit, there are enormous volumes of scientific data, including high resolution images and video, that need to be transmitted<sup>68</sup>.

Since 2023, NASA has assisted in an ongoing technological demonstration of free-space optical communications from beyond the earth-moon system. Its Deep Space Optical Communications payload, which was launched with the Psyche spacecraft, involves a DSOCC Flight Laser Transceiver, that can acquire a 1064 nm uplink laser from earth, and return a 1550 nm signal. This system includes a 22 cm unobscured optical transceiver assembly, a 4 W average power laser transmitter, actuators, sensors, electronics and software<sup>69</sup>. This system is designed to transmit data from outer space at rates 10 to 100 times faster than the state-of-the-art radio frequency systems. Early results show a maximum downlink data-rate of 267 megabits per second –a bit rate comparable to broadband internet download speeds<sup>70</sup>.

Research into optical satellite communication has focused on devices operating in the short-wave infrared (800–170 nm), thanks to the maturity and commercial availability of such components. However, longer mid-wave (3–5  $\mu\text{m}$ ) and long-wave infrared (8–14  $\mu\text{m}$ ) bands have gained the interest of investigators due to reduced atmospheric losses. Flannigan et al. have comprehensive-

ly reviewed this topic<sup>71</sup>, highlighting future prospects of practical demonstrations.

Intra-satellite communications can also benefit from integrated photonics for high-speed data transfer among onboard subsystems. Similar to terrestrial networks, spacecraft require efficient data movement, and photonic interconnects offer high data rates while reducing signal loss. Additionally, photonics can enhance electronic operations such as mixing, signal generation, and phase shifting, improving overall system performance<sup>72</sup>. The adoption of Photonic Integrated Circuits (PICs) presents a compelling alternative to conventional electronic interconnects, significantly reducing size, weight, and power – a crucial factor for space applications, particularly for miniature satellites like CubeSats<sup>73</sup>.

A significant milestone in this field is the space qualification of laser-written waveguides, which operate at 850 nm and 1550 nm, key telecommunication wavelengths. Fabricated in borosilicate Eagle XG glass, these waveguides demonstrate state-of-the-art guiding performance<sup>74</sup>. A total of 294 integrated photonic devices were subjected to proton and  $\gamma$ -ray irradiation to simulate LEO conditions at 700 km altitude. The results confirmed that their propagation losses, waveguide birefringence, evanescent coupling, and interferometric stability remained largely unaffected. This validation establishes laser-written photonic circuits as viable candidates for satellite-based experiments, particularly in quantum communication, where satellites are essential in overcoming distance limitations imposed by fiber optic losses. Beyond quantum applications, these circuits hold promise for space-based astronomical observations, where on-chip interferometry is a key technology for high-precision imaging.

Integrated optics enables the miniaturization of optical components, including waveguides, lasers, modulators, detectors, and filters, onto a single photonic chip. By integrating these elements, complex operations such as signal modulation, amplification, and routing can be performed within a compact and stable platform, enhancing the efficiency of space communication systems<sup>22</sup>. Among these components, optical modulators play a critical role in deep-space communication, encoding data, imagery, and telemetry onto radio or laser signals for inter-satellite transmission or communication with Earth<sup>75</sup>. Given the harsh space environment, modulators must be radiation-resistant, reliable, and capable of withstanding extreme thermal fluctuations<sup>76</sup>. Technologies

such as electro-optic and acousto-optic modulators significantly enhance deep-space missions, as laser-based communication offers high bandwidth and minimal signal attenuation. As future missions expand toward interplanetary exploration and human colonization, modulators will remain essential for real-time communication, remote sensing, and high-speed data transmission<sup>77</sup>.

Free Space Optical (FSO) communication represents a high-data-rate alternative to radio-frequency links for future space communication systems. However, atmospheric turbulence introduces significant challenges, degrading signal quality and limiting performance. To address this, a photonic integrated circuit (PIC) for turbulence mitigation has been developed, capable of coherently combining 32 input optical signals into a single output fiber. Fabricated using a low-loss, high-density silicon-on-insulator (SOI) process, this device integrates 31 Mach-Zehnder Interferometers (MZIs) and 31 Germanium photodetectors, achieving a bandwidth exceeding 80 kHz. The system is designed for LEO-ground and horizontal FSO links, with further developments underway to scale up to 64 input channels and reduce insertion losses<sup>78</sup>.

A complementary advancement is a self-adaptive integrated photonic receiver, designed to mitigate turbulence effects in FSO communication. Using a silicon photonic chip with a 2D Optical Antenna Array (OAA) and a Programmable Optical Processor (POP) based on MZIs, the system can coherently combine distorted wavefronts in real-time, mitigating scintillation-induced fading and improving overall signal integrity. Experimental results at 10 Gbit/s demonstrate an 8.7 dB power improvement under simulated turbulence conditions, ensuring stable data transmission. Compared to conventional solutions, this compact, energy-efficient receiver offers low latency, high scalability, and seamless compatibility with fiber optics, making it particularly suited for satellite communications, LiDAR, and quantum networking<sup>79</sup>.

### Structural health monitoring

In the early days, the only method to monitor and manage a fleet was through log hours and landing cycles, which meant that an aircraft would retire after reaching a certain pre-determined limit. As science progressed, a link between load cycles, fatigue and stress with structural damage was established, and a general understanding that flight hours are not the only relevant factor in

structure health was achieved<sup>80</sup>.

Nowadays, these concerns have culminated in the concept of Structural Health Monitoring (SHM), which aims at continuously scrutinizing the health status of the structures<sup>81</sup>, in order to improve reliability, safety, and ultimately maintenance costs<sup>19</sup>. Effective structural health monitoring leading to early detection of structure deterioration allows a proper and timely repair of the damage before it becomes irreparable, which ends up extended the safe life of the materials.

The use of advanced composite materials in aerospace engineering also entails the progress in the methods to evaluate material defects or damage, the most typical of which are delaminations, when there is a separation between two or more layers of the material (often due to residual stresses during the manufacturing phase or due to low-velocity impacts during machining or in-service) and debondings, which describe extensive separation between two elements, typically between the stiffener and the skin<sup>82</sup>.

### Optical fiber-based structural health monitoring

Optical fiber strain sensors are capable of detecting changes in strength and stiffness as a result of damage occurring to the materials, by a change in their optical properties, such as intensity, wavelength, phase or state of polarization, following a linear relation with the mechanical strain<sup>83</sup>. More specifically, FBGs are a proven approach in providing excellent solutions for a variety of structural health monitoring problems, owing to their low weight, immunity for electromagnetic interference and multiplexing capabilities. In addition, they can be either bonded to the surface of a composite or embedded within the material.

Under the scope of the UK's "CONSTRUCT" and "Integrated Wings" projects, an FBG based system has been developed for in-flight monitoring, focusing on the harsh conditions of a composite wingbox. The system operated by monitoring acoustic emission to assess damage, and load monitoring to predict the remaining lifetime. In addition, leveraging the inherent capabilities of these sensors, multiplexed sensors for strain and temperature were developed<sup>84</sup>.

There are also reports of application in unmanned aircraft's wings, with research focusing on the calibration of a measurement system capable of monitoring cross-sectional forces and moments, that included both electrical resistance and FBG strain gauges. The calibration

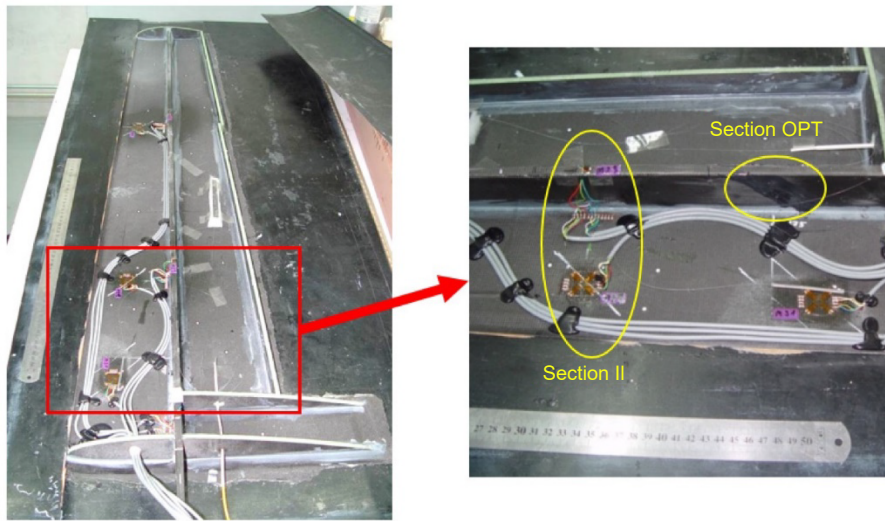


**Fig. 6 |** FBG strain gauges integrated into a wing structure. Figure reproduced with permission from ref.<sup>85</sup>, under a Creative Commons Attribution License.

allowed a comparison between the results for the complete system, consisting of three sensor units, and for various combinations of separated measuring points. A system built from only the gauges embedded in the wing spar caps enables measurements with accuracies sufficient to assess the behavior of the structure during operation (Fig. 6)<sup>85,86</sup>.

Measurement of vibrations plays a crucial role in modern engineering applications, serving as an essential diagnostic tool for detecting potential structural anomalies and ensuring the safety and reliability of various systems. Unwanted vibrations often signal damage within a system, which makes their detection vital for predictive maintenance and fault prevention. Among the various techniques explored for vibration monitoring, FBGs have emerged as a highly effective sensing technology due to their high sensitivity, immunity to electromagnetic interference, and wide frequency response range<sup>87</sup>. A recent study by Vedova et al. introduced an FBG-based vibration sensor designed specifically for the extreme conditions encountered in aerospace environments<sup>88</sup>. Their prototype consists of FBGs affixed to a cantilever-type beam, where mechanical vibrations induce an inertial load on the beam, leading to strain variations in the embedded FBGs and corresponding shifts in the Bragg wavelength. This system operated on frequencies between 0 Hz and 350 Hz. To enhance sensitivity, structural supports can be designed to resonate at specific frequencies, amplifying the induced strain and improving detection capabilities<sup>89</sup>. The performance of various sen-

sor configurations was systematically analyzed through a combination of numerical simulations and experimental validation using conventional sensors such as strain gauges and accelerometers. These comparative studies provided valuable insights into the strengths and limitations of different designs, paving the way for further optimizations in FBG-based vibration sensing technologies.

Acceleration sensors are essential for vibration monitoring in structural health assessment and environmental safety. Compared to traditional electrical accelerometers, FBG-based sensors provide higher sensitivity, lower noise, broader frequency response, and immunity to electromagnetic interference, making them a compelling alternative. A recent study proposed a low-frequency FBG acceleration sensor with a flexible hinge, spring support, and symmetric compensation mechanism to improve low-frequency detection<sup>90</sup>. The sensor's resonant frequency and sensitivity were modeled and optimized through finite element simulations, initially predicting 383.6 Hz resonance and 82.9 pm/g sensitivity. However, experimental tests revealed deviations, with a natural frequency of 73 Hz and sensitivity of 24.24 pm/g, likely due to excitation system constraints. While these results remain within acceptable limits, enhancing fabrication precision and material purity is necessary for improved performance, miniaturization, and broader applicability in aerospace and precision sensing.

Barely visible impact damage (BVID) poses significant risks to the integrity of carbon fiber reinforced polymer (CFRP) aerospace components. BVIDs typically

result from impacts such as tool drops, bird strikes, or lightning, leading to localized fiber or matrix cracking. Although a BVID may only manifest as a subtle 0.3 mm dent on the outside of the material, a substantially larger delaminated area can occur between the different plies, which can propagate under structural loads, potentially leading to component failure. Surface mounted optical fiber sensors have demonstrated the capability to monitor BVIDs over regions up to 34–46 mm wide for thermoset, and more than 70 mm for thermoplastic material systems. BVID detection on larger components can therefore be considered with a sensor density respecting these detection ranges<sup>91</sup>.

Low-velocity impact events in CFRP structures, which frequently result in BVID, are a major concern due to the reduction in strength and stiffness that may follow. Accurate detection and localization of impact events, including their severity, would represent a critical advancement for aerospace SHM applications. This, in turn, would enable more targeted inspection programs, significantly reducing the time and cost of routine maintenance. Strain measurement has been identified as an efficient method for assessing the impact response of a structure<sup>92</sup>. To support this, the current work proposes a Least Squares-Support Vector Regression (LS-SVR) algorithm to localize impact events on a CFRP plate, determining their  $X$  and  $Y$  coordinates and energy. The LS-SVR model is benchmarked against other algorithms in the literature, highlighting its effectiveness in impact localization.

A novel impact localization approach for CFRP structures is also presented in the literature, using FBG sensors paired with narrow-band laser demodulation technology. Wavelet packet decomposition is employed to extract frequency band signals, with impact energies calculated subsequently. Results indicate an average localization error of 14.2 mm, with a training time of 0.7 s<sup>93</sup>. Another method applies FBG sensors to acquire impact signals, with the frequency spectrum analyzed using a Fast Fourier Transform (FFT), providing an effective approach for low-energy impact localization<sup>94</sup>.

For detecting disbond in CFRP double-lap joints, an innovative diagnostic method was developed using FBG sensors embedded near the bondline. The FBG sensors, experiencing step-like strain distributions, could differentiate between intact and disbanded regions. As disbond grew under cyclic loading, the sensors exhibited dual reflection peaks, with the shorter wavelength peak

corresponding to the unloaded region. The gradual increase in the intensity ratio between these peaks effectively tracked the progression of disbond length, providing a quantifiable means of assessing damage<sup>95</sup>, with a resolution of approximately 2 mm.

Another significant contribution is the development and validation of specialty-coated FBG sensors for permanent installation on aerospace-grade composites, assessing their compatibility under realistic in-flight conditions. These sensors were thoroughly tested for response consistency before and after exposure to conditions such as temperature and pressure cycling, humidity, hydraulic fluid exposure, and fatigue loading, in line with aerospace standards. Results showed negligible impact on both bond line integrity and sensor signal quality, supporting the feasibility of FBG sensors for SHM of aerospace-grade composite materials<sup>96</sup>.

These collective advancements demonstrate a promising future for impact detection and monitoring in CFRP aerospace structures. Through a combination of innovative sensor technologies and advanced data analysis techniques, these methods offer practical solutions to the challenges of BVID detection and localization, thereby enhancing the reliability and safety of aerospace components.

### **Optical coherence tomography for structural health monitoring**

Optical coherence tomography (OCT) is a non-contact sensing tool, often considered analogous to ultrasound, which operates based on the principle of low coherence interferometry<sup>97</sup>, and relies on time delays and magnitude of light echoes to generate images with microscopic resolutions<sup>98</sup>. Briefly, laser light is split into two paths: the reference (with a mirror) and the object (with the sample). Light from the object path, after either being back reflected or backscattered by the structure of the sample, recombines with the light reflected in the reference path, and this interference can be detected by a photodetector unit<sup>99,100</sup>.

Ever since its debut in 1991, OCT imaging has found many applications in medicine, but it has truly revolutionized clinic ophthalmology<sup>101</sup>. It is currently used as a routine clinical tool in the diagnosis and monitorization of several eye diseases<sup>99</sup>, given the eye's highly transparent and low scattering structures<sup>102</sup>. This success reflects the technological developments from the last two decades, especially the emergence of frequency domain

OCT, which drastically increased the imaging speed and sensitivity when compared to time domain OCT<sup>103</sup>. As technology continues to evolve, increasingly more complex systems can be designed, and more applications can be explored.

Given its non-invasive nature, OCT imaging is especially useful for non-destructive testing (NDT). The ability to measure layer thickness, and detect surface and sub-surface defects such as cracks, inclusions or delaminations without damaging the object is an outstanding feature of NDT techniques<sup>104</sup>. This is particularly useful for the aerospace industry, where composites are being increasingly employed<sup>105</sup>. Because of their semitransparent property, OCT could be an ideal tool to inspect the internal structures of these materials. It is still a challenge, however, to accurately determine crack lengths, or obtain 3D crack surface profiles, which are of great importance to better understand the properties and limitations of these materials<sup>106</sup> to ultimately avoid structural failures that could result in catastrophic repercussions<sup>107</sup>. OCT, which allows depth sectioning, has previously been applied to

study delamination cracks in glass and carbon fiber composites, showing promising initial results (Fig. 7)<sup>106</sup>.

As early as 2012, Ping Liu et. al aimed to expand OCT applications beyond the biomedical field and into the aerospace industry. They developed an OCT system, using a broad bandwidth light source with center wavelength of 1550 nm, to evaluate the quality of aerospace materials, including epoxy coatings and glass fiber composites<sup>108</sup>. This system was capable of evaluating thickness and homogeneity. This research has been extended to evaluate the effects of different signal processing methods in the overall performance of the OCT system<sup>109</sup>. These developments allowed this team to later apply an OCT system to analyze samples of a glass fiber composite and study their delamination under a tensile loading. The cross-sectional images clearly show the microstructure and the crack within the specimen. The 3D crack profiles show the application of OCT to determine the evolution of the crack structure inside the composite material<sup>110,111</sup>. They also characterize polymers and polymer composites using a hybrid OCT system that coupled time-domain

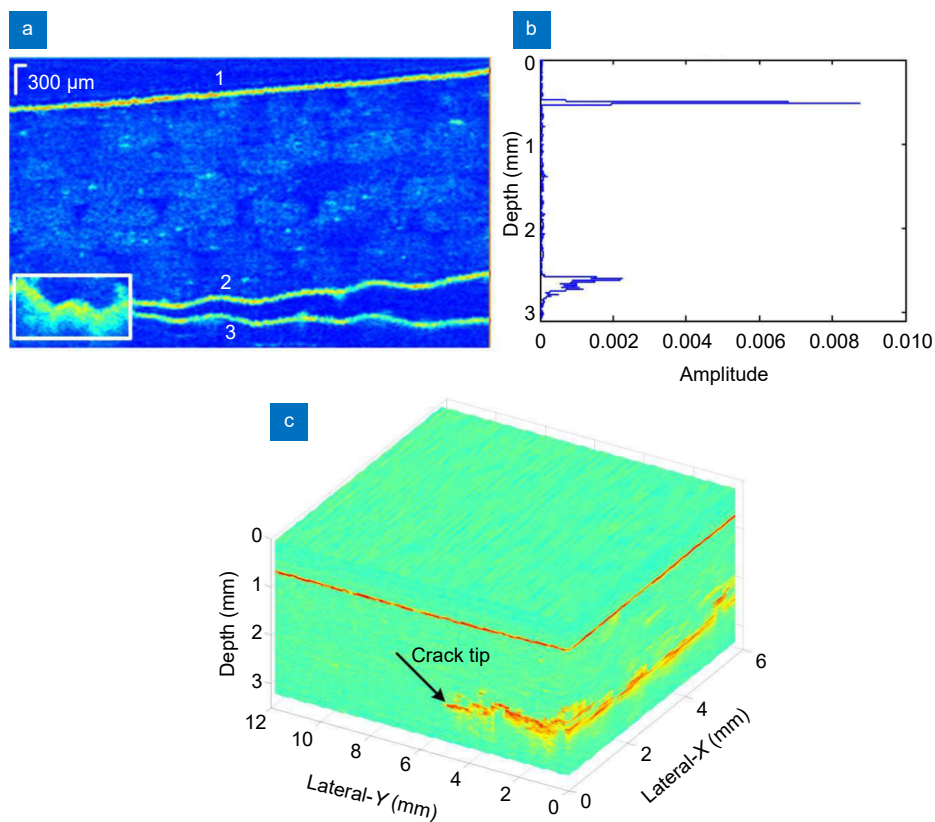


**Fig. 7** | OCT images from a delaminated glass fiber composite test after inflicted damage. (a) A cross-sectional perspective: 1) specimen surface, 2 and 3) reflections from upper and lower surfaces of the crack. White square: frontiers of the delamination crack. (b) Depth scan signal across the middle of the white square in (a). (c) Volumetric image reconstruction, highlighting the crack tip. Figure reproduced with permission from ref.<sup>106</sup>, under a Creative Commons Attribution-NoDerivs License.

OCT (TD-OCT) and Fourier-domain OCT (FD-OCT) into one system<sup>112</sup>. TD-OCT can take advantage of a large axial scan range while FD-OCT has superior performance in fast imaging as no axial scan is needed.

Wenninger et al. demonstrated the successful application of OCT to detect production defects in glass-fiber-reinforced unidirectional tapes with a thermoplastic polycarbonate matrix. Specifically, OCT was employed to identify common defects, such as dry fiber regions, empty gaps, and fiber breakage, highlighting its potential utility for quality assurance in composite manufacturing processes<sup>113</sup>.

OCT has emerged as a powerful tool for material characterization, offering valuable insights into internal structures, which are essential for both quality control and the development of new materials across industrial and medical fields. Technological advancements have significantly expanded the use of OCT in non-destructive testing (NDT), with enhanced capabilities in terms of faster image acquisition and higher resolution<sup>114</sup>. A notable advancement in OCT technology is the Master/Slave (MS) approach, which offers several benefits over conventional Fast Fourier Transform (FFT)-based OCT, including the elimination of pre-processed data and a more balanced dispersion within the interferometer. These features make MS-enhanced OCT an excellent candidate for NDT applications where flexibility is needed, particularly concerning lateral resolution and axial imaging range<sup>115</sup>.

However, a key limitation of OCT is its shallow imaging depth, constrained by the scattering of light through inhomogeneous media. The imaging depth typically ranges from several hundred microns to a few millimeters, depending on the properties of the sample, optical probing scheme, and wavelength. Since scattering losses

are inversely proportional to the wavelength of light in relation to the size of the scattering features, it has been recognized that longer center wavelengths could enhance penetration depth. Current state-of-the-art OCT systems, such as those used in dermatology, often operate at a wavelength of 1.3  $\mu\text{m}$  due to favorable factors like low water absorption and the well-developed optical components from telecommunications. Although extending OCT to longer wavelengths may theoretically increase penetration depth, this comes with challenges. Light sources and detectors become less efficient at longer wavelengths, and there is a significant increase in water absorption and vibrational absorption bands in many materials, complicating the assessment of potential imaging benefits<sup>116</sup>.

OCT has also been effectively utilized to differentiate between ductile and brittle fractures in metallic materials<sup>117,118</sup>. These studies demonstrated the potential of OCT in analyzing fractures in critical metallic parts, which could lead to catastrophic failures in aviation, maritime, automotive, or rail industries. Additionally, the prospect of a mobile OCT unit equipped with a handheld scanning probe for *in-situ* fracture analysis was discussed, providing a flexible solution for real-time assessment of damaged components.

Further demonstrating the versatility of OCT, it has been combined with other inspection techniques for enhanced defect evaluation. One notable example is the integration of OCT with terahertz pulsed imaging to assess defects in thermal barrier coatings (TBCs), which are commonly applied to aero-engine turbine blades. During engine operation, these coatings can be damaged by high temperatures and strong impact forces, leading to delamination and peeling. The combination of OCT and terahertz imaging provided a comprehensive assessment

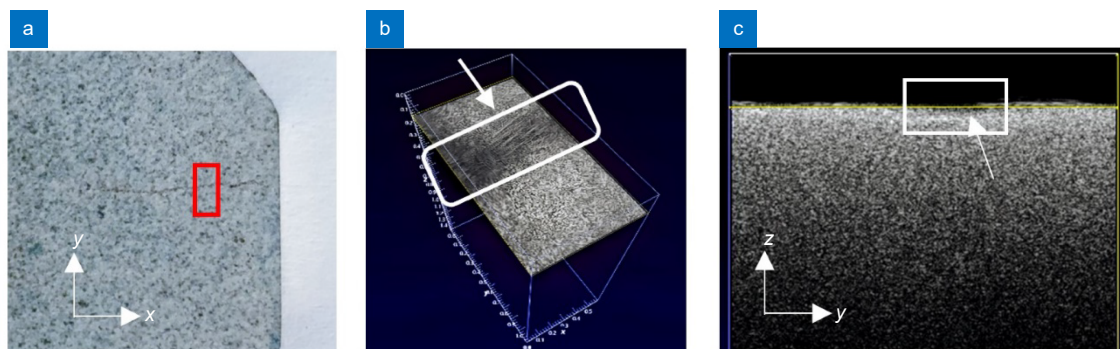


**Fig. 8 |** Scanning images showing multiple perspectives of high-temperature oxidation cracks. (a) High-temperature oxidation crack on the OCT sample table; the red box is the scanning area of the picture. (b) Near the focal point of 3D OCT imaging of the sample. (c) Volume standard OCT imaging of the sample. Figure reproduced with permission from ref.<sup>119</sup>, under a Creative Commons Attribution License.

of the TBC's integrity, both internally and externally<sup>119</sup>, making it possible to detect defects with 100  $\mu\text{m}$  width at 519  $\mu\text{m}$  depth.

Frausto-Rea et al. developed an innovative dual optical configuration to inspect the mechanical response of composite specimens made from poly-methyl-methacrylate reinforced with metallic particles. This configuration utilized digital holographic interferometry for surface data and Fourier domain OCT for internal inspection, demonstrating the power of combining complementary techniques to provide a more comprehensive analysis of composite materials<sup>120</sup>.

Overall, these developments emphasize the expanding role of OCT in NDT and material evaluation in a wide range of applications, from quality control in manufacturing to in-depth structural analysis in critical safety sectors.

### Optical monitoring of astronauts' health

Space is a harsh environment which exposes astronauts to unique health challenges. Some of the most prominent examples are body fluid redistribution, muscle atrophy and loss of bone density, which can be attributed to microgravity<sup>121</sup>, while the enhanced exposure to radiation can pose a higher risk for neurodegenerative diseases and cancer<sup>122</sup>. Since access to medical equipment

and specialized personnel is very limited, the future prospect of longer stays in space highlights the need for health monitoring tools that are simple, require minimal bulk, and allow the astronauts autonomy while performing the measurements. In this sense, breath analysis has emerged as a promising field, due to the vast information that can be obtained through it, and its inherently non-invasive nature. In fact, NASA has already developed a breath analysis system for space applications. NASA's Portable Unit for Metabolic Analysis (PUMA) is a wearable device that included a breathing mask, capable of quantifying fatty acid and carbohydrate oxidation rates,  $\text{O}_2$ , and  $\text{CO}_2$ <sup>123</sup>. The latter could be quantified through an optical sensor based on NDIR spectroscopy. Silva et al. highlighted multiple optical based sensors capable of detecting other substances, such as acetone<sup>124</sup>, ammonia<sup>125</sup>, methane<sup>126</sup>, and their potential to be applied in aerospace applications.

In-flight clinical decision-making can benefit from immediate and abundant diagnostic information, available from drops of blood or other biological specimens that can be easily and frequently obtained. measure a broad range of test classes, such as blood counts, hormones, chemistry, enzymes, nucleic acid, proteins, and biomarkers. Furthermore, cytometry can allow for high levels of assay multiplexing, allowing simultaneous measurement

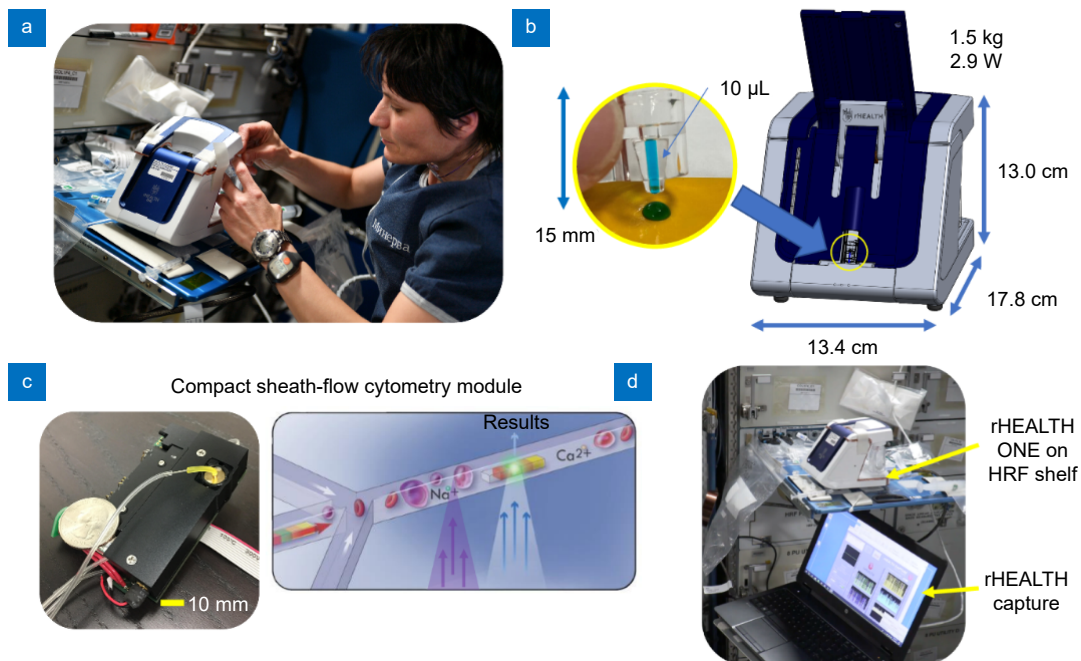


**Fig. 9** | Overview of the rHEALTH ONE experiment on the ISS. (a) The rHEALTH ONE during device setup at the ISS. (b) Detail of the sample positioning on the device. (c) Sheath-flow cytometry module, with diagram of particle analysis through the two lasers (405 nm and 532 nm). (d) On-orbit test runs. Figure reproduced with permission from ref.<sup>127</sup>, under a Creative Commons Attribution License.

of diagnostic and biological parameters, thus increasing the throughput and content of each sample analysis. Recently, Rea et al. reported the demonstration of a miniature cytometry-based analyzer (rHEALTH ONE) on the ISS<sup>127</sup>. Amongst other specific spaceflight modifications, this system was customized to fit the limited size, weight and power restrictions, while relying on alignment-free optics for surviving rocket launch. Each sample was analyzed by two lasers (405 nm and 532 nm), and the number of photons collected by the five detectors in 10  $\mu$ s intervals could be accessed through the rHEALTH Capture software program. When compared to the ground-based benchmark Gallios cytometer, this approach utilized 517 $\times$  less power, 183 $\times$  less volume, 92 $\times$  less mass, and 166 $\times$  smaller sheath reservoir. This demonstration provided a significant step forward for on-orbit biomedical analysis.

Another significant issue caused by the microgravity environment is the incidence of Spaceflight associated neuro-ocular syndrome (SANS), which refers to the unique neuro-ophthalmic findings that have been described in astronauts during and after long-duration spaceflight. The imaging and clinical findings of SANS include optic disc oedema (ODE), chorioretinal folds, hyperopic refractive shift, posterior globe flattening, and total retinal and retina nerve fiber layer thickening<sup>128</sup>. To further understand this issue, Patel et al. studied the changes in the optical nerve head and surrounding tissue using preflight and postflight OCT scans from ISS astronauts<sup>129</sup>.

Additionally, it is worth noting that OCT has already been performed in space. In fact, in 2013, NASA deployed the Heidelberg Spectralis OCT to the ISS<sup>130</sup>. The crew had OCT baseline examinations prior to their missions on space, and the follow-up examinations intend to register and monitor ocular changes throughout long term missions. More recently, a Heidelberg Spectralis "OCT2" device has been activated on the ISS<sup>131</sup>. This updated system represents an increase in sensitivity, offering enhanced resolution and depth imaging, on top of being more user-friendly. These advances provide the basis for a better future understanding of SANS, which NASA has considered as one of the highest priority risks to astronauts in space.

## Final remarks

Given the expected increase in aerospace activity in the coming years, the development and integration of new

and improved technologies is essential to continue to make these explorations easier and more effective. The inherent advantages of using optical technologies such as the resilience to harsh environments and the ability to construct lightweight systems, while maintaining a high level of precision –position them as transformative solutions to modernize the aerospace industry.

This review has highlighted numerous remarkable contributions to aerospace applications, showcasing a diverse range of optical sensors and systems tailored for the field. While some innovations have already been adopted for operational use, many more are still in experimental stages, requiring further refinement to meet the rigorous industry demands. Despite the significant progress made, some challenges still remain. Miniaturization of components, enhanced resistance to the harsh operating conditions, and the integration of optical systems with artificial intelligence for autonomous decision-making are areas that require more intensive research and development. Furthermore, the interest in achieving a more sustainable exploration, alongside the need to reduce the vehicles' weight and energy consumptions, will continue to drive innovation and evolution.

Addressing these gaps will be essential to ensure optical systems can fully meet the complex requirements of future aerospace missions, especially as activities extend far beyond Earth's orbit, hopefully leading to a more widespread adoption in real-world missions.

Future trends in aerospace optical systems are moving towards a highly integrated, multidisciplinary approach that leverages emerging technologies such as nanophotonics, machine learning, and additive manufacturing. Nanophotonics promises unprecedented miniaturization and enhanced performance through the use of sub-wavelength structures and metamaterials, which can lead to more compact and efficient optical components. Concurrently, machine learning techniques are being employed to optimize optical design parameters, automate calibration and fault detection processes, and enhance real-time data processing, thereby streamlining the development and operation of these systems. Additive manufacturing is set to revolutionize the production of optical components by enabling the fabrication of customized, lightweight parts with complex geometries that traditional manufacturing methods cannot achieve. These innovations are expected to drive significant advancements in key aerospace applications, including earth observation, deep-space exploration, and in-space

manufacturing. Moreover, the development of novel materials and advanced coatings will be critical to improving the durability and performance of optical systems under harsh space conditions such as extreme temperatures, radiation, and mechanical stress. As the aerospace industry continues to expand its capabilities, these cutting-edge technologies will play an increasingly vital role in enabling more resilient, efficient, and cost-effective optical solutions that are essential for future missions and for deepening our understanding of the universe.

In conclusion, multiple technologies have demonstrated great promise, thus continued investment in research and development, strong interdisciplinary collaborations, and industry-standardization efforts are critical to unlock their full potential towards full-scale adoption and optimization.

## References

- Sause MGR, Jasiūnienė E. *Structural Health Monitoring Damage Detection Systems for Aerospace* (Springer, Cham, 2021). <http://doi.org/10.1007/978-3-030-72192-3>.
- Oyewo AT, Oluwole OO, Ajide OO et al. A summary of current advancements in hybrid composites based on aluminium matrix in aerospace applications. *Hybrid Adv* 5, 100117 (2024).
- Blakey-Milner B, Gradl P, Snedden G et al. Metal additive manufacturing in aerospace: a review. *Mater Des* 209, 110008 (2021).
- Agarwal RK. Grand challenges in aerospace engineering. *Front Aerosp Eng* 3, 1383934 (2024).
- Irving PE, Soutis C. *Polymer Composites in the Aerospace Industry* 1–520 (Elsevier, Amsterdam, 2014). <http://doi.org/10.1016/C2013-0-16303-9>.
- Ciampa F, Mahmoodi P, Pinto F et al. Recent advances in active infrared thermography for non-destructive testing of aerospace components. *Sensors* 18, 609 (2018).
- Rana S, Fanguero R. Advanced composites in aerospace engineering. In Rana S, Fanguero R. *Advanced Composite Materials for Aerospace Engineering* 1–15 (Elsevier, Amsterdam, 2016). <http://doi.org/10.1016/B978-0-08-100037-3.00001-8>.
- Li Y, Xiao Y, Yu L et al. A review on the tooling technologies for composites manufacturing of aerospace structures: materials, structures and processes. *Compos Part A: Appl Sci Manuf* 154, 106762 (2022).
- Hegde G, Asokan S, Hegde G. Fiber Bragg grating sensors for aerospace applications: a review. *ISSS J Micro Smart Syst* 11, 257–275 (2022).
- Mckenzie I, Ibrahim S, Haddad E et al. Fiber optic sensing in spacecraft engineering: an historical perspective from the European space agency. *Front Phys* 9, 719441 (2021).
- Anwar A, Albano M, Hassan G et al. Vacuum effect on spacecraft structure materials. *Int Conf Aerosp Sci Aviat Technol* 16, 1–10 (2015).
- Newman DJ. Life in extreme environments: how will humans perform on Mars. *Gravit Space Biol Bull* 13, 35–47 (2000).
- Townsend LW, Fry RJM. Radiation protection guidance for activities in low-earth orbit. *Adv Space Res* 30, 957–963 (2002).
- Mespoulet J, Hérel PL, Abdulhamid H et al. Experimental study of hypervelocity impacts on space shields above 8 km/s. *Procedia Eng* 204, 508–515 (2017).
- Di Sante R. Fibre optic sensors for structural health monitoring of aircraft composite structures: recent advances and applications. *Sensors* 15, 18666–18713 (2015).
- Li J, Wang LW, Guo Y et al. Study on aberration correction of adaptive optics based on convolutional neural network. *Photonics* 8, 377 (2021).
- Cheng XM, Yang YK, Hao Q. Analysis of the effects of thermal environment on optical systems for navigation guidance and control in supersonic aircraft based on empirical equations. *Sensors* 16, 1717 (2016).
- Jiao ZL, Jiang LX, Sun JP et al. Outgassing environment of spacecraft: an overview. *IOP Conf Ser Mater Sci Eng* 611, 012071 (2019).
- Rovera A, Tancau A, Boetti N et al. Fiber optic sensors for harsh and high radiation environments in aerospace applications. *Sensors* 23, 2512 (2023).
- Ince JC, Peerzada M, Mathews LD et al. Overview of emerging hybrid and composite materials for space applications. *Adv Compos Hybrid Mater* 6, 130 (2023).
- Finckenor MM, de Groh KK. *A Researcher's Guide to: Space Environmental Effects* (2020).
- Butt MA. Integrated optics: platforms and fabrication methods. *Encyclopedia* 3, 824–838 (2023).
- Sposito A, Pechstedt RD. Optical sensors for aerospace applications: brake temperature sensors and fuel pump pressure sensors for aircraft. In *2016 IEEE Metrology for Aerospace (MetroAeroSpace)* 97–101 (IEEE, 2016). <http://doi.org/10.1109/MetroAeroSpace.2016.7573193>.
- Raj AB, Majumder AK. Historical perspective of free space optical communications: from the early dates to today's developments. *IET Commun* 13, 2405–2419 (2019).
- Cao JJ, Chang J, Huang Y et al. Optical design and fabrication of a common-aperture multispectral imaging system for integrated deep space navigation and detection. *Opt Lasers Eng* 167, 107619 (2023).
- Sung K, Peck C, Majji M et al. An optical navigation system for autonomous aerospace systems. *IEEE Sens J* 22, 16862–16873 (2022).
- Silvestrini S, Piccinin M, Zanotti G et al. Optical navigation for Lunar landing based on convolutional neural network crater detector. *Aerosp Sci Technol* 123, 107503 (2022).
- Theil S, Ammann N, Andert F et al. ATON (Autonomous Terrain-based Optical Navigation) for exploration missions: recent flight test results. *CEAS Space J* 10, 325–341 (2018).
- Ho HW, de Croon GCHE, Chu QP. Distance and velocity estimation using optical flow from a monocular camera. *Int J Micro Air Veh* 9, 198–208 (2017).
- Franzese V, Topputo F. Deep-space optical navigation exploiting multiple beacons. *J Astronaut Sci* 69, 368–384 (2022).
- Franzese V, Topputo F, Ankersen F et al. Deep-space optical navigation for M-ARGO mission. *J Astronaut Sci* 68, 1034–1055 (2021).
- Andreis E, Franzese V, Topputo F. An overview of autonomous optical navigation for deep-space CubeSats. In *72nd International Astronautical Congress (IAC)* 25–29 (IAF, 2021).
- Negro J, Griffin SF, Kelchner BL et al. Inertial stable platforms for precision pointing of optical systems in aerospace applications. *AIAA J* 61, 3234–3246 (2023).
- Spytek J, Ambrozinski L, Pelivanov I. Non-contact detection of ultrasound with light – review of recent progress. *Photoacous-*

- tics* 29, 100440 (2023).
35. Xu H, Wang L, Zu YT et al. Application and development of fiber optic gyroscope inertial navigation system in underground space. *Sensors* 23, 5627 (2023).
  36. Nayak J. Fiber-optic gyroscopes: from design to production [invited]. *Appl Opt* 50, E152–E161 (2011).
  37. Mckenzie I, Karafolas N. Fiber optic sensing in space structures: the experience of the European space agency (invited paper). *Proc SPIE* 855, 262–269 (2005).
  38. Korkishko YN, Fedorov VA, Prilutskiy VE et al. Space grade fiber optic gyroscope: R&D results and flight tests. In *2016 DGON Inertial Sensors and Systems (ISS)* 1–19 (IEEE, 2016). <http://doi.org/10.1109/InertialSensors.2016.7745682>.
  39. Prins JJM. SLOSHSAT FLEVO facility for liquid experimentation and verification in orbit. (2000). <http://hdl.handle.net/10921/890> (accessed September 10, 2024).
  40. Girard S, Morana A, Ladaci A et al. Recent advances in radiation-hardened fiber-based technologies for space applications. *J Opt* 20, 093001 (2018).
  41. Nunes GFS, Sakamoto JMS. Passive interferometric fiber-optic gyroscope for aerospace applications. In *2024 Latin American Workshop on Optical Fiber Sensors (LAWOFS)* 1–2 (IEEE, 2024). <http://doi.org/10.23919/LAWOFS62242.2024.10560851>.
  42. Sakamoto J, Fernandes G, Silva R et al. Development of a fiber optic inertial measurement unit for space applications. In *2024 SBFoton International Optics and Photonics Conference (SBFoton IOPC)* 1–5 (IEEE, 2024). <http://doi.org/10.1109/SBFotonIOPC62248.2024.10813470>.
  43. Kabashima S, Ozaki T, Takeda N. Structural health monitoring using FBG sensor in space environment. *Proc SPIE* 4332, 78–87 (2001).
  44. Azhari A, Liang R, Toyserkani E. A novel fibre Bragg grating sensor packaging design for ultra-high temperature sensing in harsh environments. *Meas Sci Technol* 25, 075104 (2014).
  45. Ma SN, Xu YP, Pang YX et al. Optical fiber sensors for high-temperature monitoring: a review. *Sensors* 22, 5722 (2022).
  46. Yang S, Hu D, Wang AB. Point-by-point fabrication and characterization of sapphire fiber Bragg gratings. *Opt Lett* 42, 4219–4222 (2017).
  47. Ivanov OV, Caldas P, Rego G. High sensitivity cryogenic temperature sensors based on arc-induced long-period fiber gratings. *Sensors* 22, 7119 (2022).
  48. Aimasso A, Dalla Vedova MDL, Maggiore P et al. Study of FBG-based optical sensors for thermal measurements in aerospace applications. *J Phys Conf Ser* 2293, 012006 (2022).
  49. Tian Q, Xin GG, Lim KS et al. Optical fiber sensor with double tubes for accurate strain and temperature measurement under high temperature up to 1000 °C. *IEEE Sens J* 22, 11710–11716 (2022).
  50. Liao T, Pei YF, Xu J et al. Fiber Bragg grating temperature sensors applied in harsh environment of aerospace. In *2018 Asia Communications and Photonics Conference* 1–3 (IEEE, 2018). <http://doi.org/10.1109/ACP.2018.8595842>.
  51. Abad S, Araújo FM, Pedersen F et al. Applications of FBG sensors on telecom satellites. *Proc SPIE* 10565, 1056517 (2017).
  52. Nannipieri P, Meoni G, Nesti F et al. Application of FBG sensors to temperature measurement on board of the REXUS 22 sounding rocket in the framework of the U-PHOS project. In *2017 IEEE International Workshop on Metrology for AeroSpace* 462–467 (IEEE, 2017). <http://doi.org/10.1109/METROAEROSPACE.2017.7999618>.
  53. Meyer A, Morana A, Weninger L et al. Toward an embedded and distributed optical fiber-based dosimeter for space applications. *IEEE Trans Nucl Sci* 70, 583–589 (2023).
  54. Di Francesca D, Balcon N, Cheiney P et al. Low radiation dose calibration and theoretical model of an optical fiber dosimeter for the international space station. *Appl Opt* 62, E43–E50 (2023).
  55. Meyer ME, Urban DL, Mulholland GW et al. Evaluation of spacecraft smoke detector performance in the low-gravity environment. *Fire Saf J* 98, 74–81 (2018).
  56. Terracciano AC, Thurmond K, Villar M et al. Hazardous gas detection sensor using broadband light-emitting diode-based absorption spectroscopy for space applications. *New Space* 6, 28–36 (2018).
  57. Fradet M, Bendig RM, Briggs RM. The combustion product monitor instrument for the spacecraft fire safety demonstration project. In *49th International Conference on Environmental Systems (ICES)* (JPL Open Repository, 2019).
  58. Wang XL, Zhou H, Arnott WP et al. Evaluation of gas and particle sensors for detecting spacecraft-relevant fire emissions. *Fire Saf J* 113, 102977 (2020).
  59. Koekemoer AM, Aussel H, Calzetti D et al. The COSMOS survey: *Hubble Space telescope* advanced camera for surveys observations and data processing. *Astrophys J Suppl Ser* 172, 196–202 (2007).
  60. Martin S, Lawrence C, Redding D et al. Next-generation active telescope for space astronomy. *J Astron Telesc Instrum Syst* 8, 044005 (2022).
  61. Butt MA. A comprehensive exploration of contemporary photonic devices in space exploration: a review. *Photonics* 11, 873 (2024).
  62. Opromolla R, Fasano G, Rufino G et al. A review of cooperative and uncooperative spacecraft pose determination techniques for close-proximity operations. *Prog Aerosp Sci* 93, 53–72 (2017).
  63. ESA. ESA space environment report 2024. [https://www.esa.int/Space\\_Safety/Space\\_Debris/ESA\\_Space\\_Environment\\_Report\\_2024](https://www.esa.int/Space_Safety/Space_Debris/ESA_Space_Environment_Report_2024) (accessed September 12, 2024).
  64. Palmer DM, Holmes RM. Extremely low resource optical identifier: a license plate for your satellite. *J Spacecr Rockets* 55, 1014–1023 (2018).
  65. Bartels N, Allenspacher P, Hampf D et al. Space object identification via polarimetric satellite laser ranging. *Commun Eng* 1, 5 (2022).
  66. Xie Y, Xie Y, Li B et al. Advancements in spaceborne synthetic aperture radar imaging with system-on-chip architecture and system fault-tolerant technology. *Remote Sens (Basel)* 15, 4739 (2023).
  67. Kaushal H, Kaddoum G. Optical communication in space: challenges and mitigation techniques. *IEEE Commun Surv Tutor* 19, 57–96 (2017).
  68. NASA. Deep space optical communications (DSOC). <https://www.nasa.gov/mission/deep-space-optical-communications-dsoc/> (accessed September 13, 2024).
  69. Biswas A, Srinivasan M, Andrews KS et al. Deep space optical communications technology demonstration. *Proc SPIE* 12877, 1287706 (2024).
  70. NASA. NASA's optical comms demo transmits data over 140 million miles. <https://www.nasa.gov/missions/psyche-mission/nasas-optical->

- [comms-demo-transmits-data-over-140-million-miles/](#) (accessed September 13, 2024).
71. Flannigan L, Yoell L, Xu CQ. Mid-wave and long-wave infrared transmitters and detectors for optical satellite communications—a review. *J Opt* **24**, 043002 (2022).
  72. Tzintzarov GN, Rao SG, Cressler JD. Integrated silicon photonics for enabling next-generation space systems. *Photonics* **8**, 131 (2021).
  73. Krainak MA, Stephen MA, Troupaki E et al. Integrated photonics for NASA applications. *Proc SPIE* **10899**, 108990F (2019).
  74. Piacentini S, Vogl T, Corrielli G et al. Space qualification of ultrafast laser - written integrated waveguide optics. *Laser Photonics Rev* **15**, 2000167 (2021).
  75. Sakuma T, Yokoyama S, Fujikata J. High performance Si and InP/EO polymer hybrid optical modulators for data communication and computing. In *Proceedings of the 2022 Conference on Lasers and Electro-Optics Pacific Rim CWP12A\_02* (Optica Publishing Group, 2022). [http://doi.org/10.1364/CLEOPR.2022.CWP12A\\_02](http://doi.org/10.1364/CLEOPR.2022.CWP12A_02).
  76. Guo M, Wang YF, Yao Y et al. Experimental demonstration of SNSPD-based free space optical communication with a high extinction ratio modulator. *Opt Commun* **550**, 129998 (2024).
  77. Mesleh R, AL-Olaimat A. Acousto-optical modulators for free space optical wireless communication systems. *J Opt Commun Netw* **10**, 515 (2018).
  78. de Marinis L, Seigo Kincaid P, Lucas Y et al. A silicon photonic 32-input coherent combiner for turbulence mitigation in free space optics links. *IEEE Access* **13**, 31718–31728 (2025).
  79. Martinez AI, Cavicchioli G, Seyedinnavadeh S et al. Self-adaptive integrated photonic receiver for turbulence compensation in free space optical links. *Sci Rep* **14**, 20178 (2024).
  80. Khana AA, Zafar S, Shafi Khan N et al. History, current status and challenges to structural health monitoring system in aviation field. *J Space Technol* **4**, 67–74 (2014).
  81. Farrar CR, Worden K. An introduction to structural health monitoring. *Philos Trans A Math Phys Eng Sci* **365**, 303–315 (2007).
  82. Güemes A, Fernandez-Lopez A, Pozo AR et al. Structural health monitoring for advanced composite structures: a review. *J Compos Sci* **4**, 13 (2020).
  83. Rocha H, Sempriroschnig C, Nunes JP. Sensors for process and structural health monitoring of aerospace composites: a review. *Eng Struct* **237**, 112231 (2021).
  84. Zhang W, Zhao L, Wang JY et al. Fiber grating sensing for aerospace applications. In *2023 21st International Conference on Optical Communications and Networks 1–3* (IEEE, 2023). <http://doi.org/10.1109/ICOCN59242.2023.10236347>.
  85. Świąch Ł. Calibration of a load measurement system for an unmanned aircraft composite wing based on fibre Bragg gratings and electrical strain gauges. *Aerospace* **7**, 27 (2020).
  86. Pei YF, Liao T, Pei YF et al. FBG strain sensor applied in harsh environment of aerospace. In *2018 IEEE 3rd Optoelectronics Global Conference (OGC)* 81–84 (IEEE, 2018). <http://doi.org/10.1109/OGC.2018.8529994>.
  87. Li TL, Guo JX, Tan YG et al. Recent advances and tendency in fiber Bragg grating-based vibration sensor: a review. *IEEE Sens J* **20**, 12074–12087 (2020).
  88. Dalla Vedova MDL, Quattrocchi G, Aimasso A et al. Rapid prototyping of FBG-based optical sensors for vibration analysis of mechatronic systems. *J Phys Conf Ser* **2698**, 012004 (2024).
  89. Quattrocchi G, Berri PC, Vedova Dalla MDL et al. Optical fibers applied to aerospace systems prognostics: design and development of new FBG-based vibration sensors. *IOP Conf Ser Mater Sci Eng* **1024**, 012095 (2021).
  90. Meng LJ, Zhu PP, Tan X et al. A low-frequency fiber Bragg grating acceleration sensor based on spring support and symmetric compensation structure with flexible hinges. *Sensors* **24**, 2990 (2024).
  91. Goossens S, Berghmans F, Sharif Khodaei Z et al. Practicalities of BVID detection on aerospace-grade CFRP materials with optical fibre sensors. *Compos Struct* **259**, 113243 (2021).
  92. Datta A, Augustin MJ, Gupta N et al. Impact localization and severity estimation on composite structure using fiber Bragg grating sensors by least square support vector regression. *IEEE Sens J* **19**, 4463–4470 (2019).
  93. Sai YZ, Zhao XX, Wang LL et al. Impact localization of CFRP structure based on FBG sensor network. *Photonic Sens* **10**, 88–96 (2020).
  94. Zhao G, Li SX, Hu HX et al. Impact localization on composite laminates using fiber Bragg grating sensors and a novel technique based on strain amplitude. *Opt Fiber Technol* **40**, 172–179 (2018).
  95. Yashiro S, Wada J, Sakaida Y. A monitoring technique for disbond area in carbon fiber-reinforced polymer bonded joints using embedded fiber Bragg grating sensors: development and experimental validation. *Struct Health Monit* **16**, 185–201 (2017).
  96. Goossens S, De Pauw B, Geernaert T et al. Aerospace-grade surface mounted optical fibre strain sensor for structural health monitoring on composite structures evaluated against in-flight conditions. *Smart Mater Struct* **28**, 065008 (2019).
  97. Fujimoto JG, Pitris C, Boppart SA et al. Optical coherence tomography: an emerging technology for biomedical imaging and optical biopsy. *Neoplasia* **2**, 9–25 (2000).
  98. Fujimoto J, Swanson E. The development, commercialization, and impact of optical coherence tomography. *Invest Ophthalmol Vis Sci* **57**, OCT1–OCT13 (2016).
  99. Drexler W, Fujimoto JG. *Optical Coherence Tomography: Technology and Applications* 2nd ed 1–2571 (Springer, Cham, 2015). <http://doi.org/10.1007/978-3-319-06419-2>.
  100. Bouma BE, de Boer JF, Huang D et al. Optical coherence tomography. *Nat Rev Methods Primers* **2**, 79 (2022).
  101. Rosenfeld PJ. Optical coherence tomography and the development of antiangiogenic therapies in neovascular age-related macular degeneration. *Invest Ophthalmol Vis Sci* **57**, OCT14–OCT26 (2016).
  102. Bouma BE, Villiger M, Otsuka K et al. Intravascular optical coherence tomography [invited]. *Biomed Opt Express* **8**, 2660–2686 (2017).
  103. Zhang ZJ, Yang XY, Zhao ZY et al. Rapid imaging and product screening with low-cost line-field Fourier domain optical coherence tomography. *Sci Rep* **13**, 10809 (2023).
  104. Zechel F, Kunze R, König N et al. Optical coherence tomography for non-destructive testing. *Tech Mess* **87**, 404–413 (2020).
  105. Hassani S, Mousavi M, Gandomi AH. Structural health monitoring in composite structures: a comprehensive review. *Sensors* **22**, 153 (2021).
  106. Liu P, Yao LJ, Groves RM. Near-infrared optical coherence tomography for the inspection of fiber composites. In *7th International Symposium on NDT in Aerospace* (AeroNDT, 2015).
  107. Nsengiyumva W, Zhong SC, Lin JW et al. Advances, limitations and prospects of nondestructive testing and evaluation of

- thick composites and sandwich structures: a state-of-the-art review. *Compos Struct* **256**, 112951 (2021).
108. Liu P, Groves RM, Benedictus R. Quality assessment of aerospace materials with optical coherence tomography. *Proc SPIE* **8430**, 84300I (2012).
109. Liu P, Groves RM, Benedictus R. Signal processing in optical coherence tomography for aerospace material characterization. *Opt Eng* **52**, 033201 (2013).
110. Liu P, Groves RM, Benedictus R. Non-destructive evaluation of delamination growth in glass fiber composites using optical coherence tomography. *Proc SPIE* **9063**, 90631M (2014).
111. Liu P, Groves RM, Benedictus R. 3D monitoring of delamination growth in a wind turbine blade composite using optical coherence tomography. *NDT & E Int* **64**, 52–58 (2014).
112. Liu P, Groves RM, Benedictus R. Optical coherence tomography for the study of polymer and polymer matrix composites. *Strain* **50**, 436–443 (2014).
113. Wenninger M, Marschik C, Felbermayer K et al. Optical coherence tomography - A new method for evaluating the quality of thermoplastic glass-fiber-reinforced unidirectional tapes. *AIP Conf Proc* **2884**, 050008 (2023).
114. Nteroli G, Podoleanu A, Bradu A. Combining photoacoustic and optical coherence tomography imaging for nondestructive testing applications. *Proc SPIE* **12170**, 121700P (2022).
115. Bradu A, Marques M, Rivet S et al. Current capabilities and challenges for optical coherence tomography as a high impact non-destructive imaging modality. *Proc SPIE* **10831**, 108310E (2018).
116. Petersen CR, Israelsen NM, Barh A et al. Mid-infrared OCT imaging in highly scattering samples using real-time upconversion of broadband supercontinuum covering from 3.6–4.6  $\mu\text{m}$ . *Proc SPIE* **10873**, 108730X (2019).
117. Hutiu G, Duma VF, Demian D et al. Surface imaging of metallic material fractures using optical coherence tomography. *Appl Opt* **53**, 5912–5916 (2014).
118. Hutiu G, Duma VF, Demian D et al. Assessment of ductile, brittle, and fatigue fractures of metals using optical coherence tomography. *Metals* **8**, 117 (2018).
119. Luo MT, Zhong SC, Huang Y et al. Combined terahertz pulsed imaging and optical coherence tomography detection method for multiple defects in thermal barrier coatings. *Coatings* **14**, 380 (2024).
120. Frausto-Rea G, De La Torre-Ibarra MH, Muñoz-Huerta RF et al. Mechanical test study in composites using digital holographic interferometry and optical coherence tomography simultaneously. *Appl Opt* **59**, 857–865 (2020).
121. Roda A, Mirasoli M, Guardigli M et al. Advanced biosensors for monitoring astronauts' health during long-duration space missions. *Biosens Bioelectron* **111**, 18–26 (2018).
122. Elias Abi-Ramia Silva T, Burisch F, Güntner AT. Gas sensing for space: health and environmental monitoring. *Trends Analyt Chem* **177**, 117790 (2024).
123. Dietrich DL, Juergens JR, Lewis ME et al. Portable unit for metabolic analysis, US-Patent-10, 076, 268, 2018. <https://ntrs.nasa.gov/citations/20180006275> (accessed September 27, 2024).
124. Bovey F, Cros J, Tuzson B et al. Breath acetone as a marker of energy balance: an exploratory study in healthy humans. *Nutr Diabetes* **8**, 50 (2018).
125. Neri G, Lacquaniti A, Rizzo G et al. Real-time monitoring of breath ammonia during haemodialysis: use of ion mobility spectrometry (IMS) and cavity ring-down spectroscopy (CRDS) techniques. *Nephrol Dial Transplant* **27**, 2945–2952 (2012).
126. Lin YY, Manalili D, Khodabakhsh A et al. Real-time measurement of  $\text{CH}_4$  in human breath using a compact  $\text{CH}_4/\text{CO}_2$  sensor. *Sensors* **24**, 1077 (2024).
127. Rea DJ, Miller RS, Crucian BE et al. Single drop cytometry onboard the international space station. *Nat Commun* **15**, 2634 (2024).
128. Ong J, Tarver W, Brunstetter T et al. Spaceflight associated neuro-ocular syndrome: proposed pathogenesis, terrestrial analogues, and emerging countermeasures. *Br J Ophthalmol* **107**, 895–900 (2023).
129. Patel N, Pass A, Mason S et al. Optical coherence tomography analysis of the optic nerve head and surrounding structures in long-duration international space station astronauts. *JAMA Ophthalmol* **136**, 193–200 (2018).
130. Lee AG, Mader TH, Gibson CR et al. Spaceflight associated neuro-ocular syndrome (SANS) and the neuro-ophthalmologic effects of microgravity: a review and an update. *NPJ Microgravity* **6**, 7 (2020).
131. Soares B, Ong J, Waisberg E et al. Imaging in spaceflight associated neuro-ocular syndrome (SANS): current technology and future directions in modalities. *Life Sci Space Res (Amst)* **42**, 40–46 (2024).

## Acknowledgements

This research was funded by National Funds through the Portuguese Science and Technology Foundation (FCT I.P.) under the scope of the project CICECO (LA/P/0006/2020, UIDB/50011/2020, UIDP/50011/2020). The research was co-funded by the financial support of the European Union under the REFRESH – Research Excellence For Region Sustainability and High-tech Industries project number CZ.10.03.01/00/22\_003/0000048 via the Operational Programme Just Transition. This work was also supported by the Ministry of Education, Youth, and Sports of the Czech Republic conducted by the VSB-Technical University of Ostrava, under grants no. SP2025/039 and SP2025/021.

## Competing interests

Carlos Marques serves as an Editor for the Journal, and no other author has reported any competing interests.



Scan for Article PDF